DET NORSKE VERITAS

Final Report
Metallurgical Analysis of Leak on Eight-Inch Diameter Moosehorn Pipeline

Pembina Pipeline Corporation
Calgary, Alberta

Report No./DNV Reg No.: ANEUS813BPADG (PP023929)
November 1, 2011

Metallurgical Analysis of Leak on Eight-Inch Diameter Moosehorn Pipeline	DET NORSKE VERITAS (U.S.A.), INC. Materials & Corrosion Technology Center 5777 Frantz Road Dublin, OH 43017-1386, United States Tel: (614) 761-1214 Fax: (614) 761-1633 http://www.dnv.com http://www.dnvusa.com
For: Pembina Pipeline Corporation 2000, 700-9 Avenue S.W. Calgary, Alberta T2P 3V4	
Account Ref.:	

Date of First Issue:	October 31, 2011	Project No.	PP023929
Report No.:		Organization Unit:	Materials & Corrosion Technology Ctr.
Revision No.:		Subject Group:	

Summary:

Please see Executive Summary.

Prepared by:	Barbara Nicole Padgett, Ph.D. Senior Engineer	*Signature*
Verified by:	John A. Beavers, Ph.D., FNACE Director – Failure Analysis	*Signature*
Approved by:	Oliver C. Moghissi, Ph.D. Director, Materials & Corrosion Technology Center	*Signature*

☑	No distribution without permission from the client or responsible organizational unit (however, free distribution for internal use within DNV after 3 years)	Indexing Terms	
☐	No distribution without permission from the client or responsible organizational unit	Key Words	
☐	Strictly confidential	Service Area	
☐	Unrestricted distribution	Market Segment	

Rev. No. / Date:	Reason for Issue:	Prepared by:	Approved by:	Verified by

© 2011 Det Norske Veritas (U.S.A.), Inc.
All rights reserved. This publication or parts thereof may not be reproduced or transmitted in any form or by any means, including photocopying or recording, without the prior written consent of Det Norske Veritas (U.S.A.), Inc.

Executive Summary

Pembina Pipeline Corporation (*Pembina*) retained Det Norske Veritas (U.S.A.), Inc. (*DNV*) to perform a metallurgical analysis on a section of pipe from the eight-inch nominal diameter Deer Mountain Lateral crude oil pipeline that leaked. The leak was discovered on August 15, 2011 near Swan Hills, Alberta at kilometer post (KP) 44.007, 12.98 m from the upstream girth weld.

The portion of the pipeline that was removed is comprised 219 mm diameter by 4.8 mm wall thickness, API 5L X42 line pipe steel that contains an electric resistance welded (ERW) longitudinal seam. The maximum operating pressure (MOP) is 8275 kPa, which corresponds to 65.5% of the specified minimum yield strength (SMYS). The normal operating pressure is 5500 kPa, which corresponds to 43.5% of SMYS.

The pipeline was installed in 1961 and was externally coated with polyethylene tape and a fiberglass outer wrap. The coating at the leak was reportedly in poor condition and contained liquid under the coating; the pH of a liquid sample was 8.5.

Following construction, a hydrostatic pressure test was performed. The pipeline has an impressed current cathodic protection (CP) system that was installed in 1961. Cathodic protection readings were taken on July 31, 2011 in the vicinity of the leak. Pipe to soil potentials were 1353 mV (on).

In the field, the coating was removed, the pipe was cleaned, and magnetic particle inspection (MPI) was performed in the vicinity of the leak location. A 3.93 m section of pipe that contained the leak was shipped to DNV for analysis. The objectives of the analysis were to determine the metallurgical cause of the failure and identify any contributing factors.

The procedures used in the analysis were in accordance with industry-accepted standards. Five of the general standards governing terminology, specific metallographic procedures, mechanical testing, and chemical analysis used are as follows:

- ASTM E7, “Standard Terminology Relating to Metallography.”
- ASTM E3, “Standard Methods of Preparation of Metallographic Specimens.”
- ASTM E8, “Test Methods for Tension Testing of Metallic Materials.”
- ASTM E23, “Standard Test Methods for Notched Bar Impact Testing of Metallic Materials.”
- ASTM A751, “Standard Test Methods, Practices, and Terminology for Chemical Analysis of Steel Products.”

The following steps were performed for this analysis. The pipe section was visually inspected and photographed. Wall thicknesses, diameters, and circumferences were measured on the pipe ends where coating was not present. Portions of the pipe that contained MPI indications were cleaned with a solvent. MPI was performed at these indications and the pipe was photographed.

Pipe samples that contained the indications (including the leak location) were removed from the pipe section, placed in liquid nitrogen, and hit with a hammer to reveal the fracture surfaces. The fracture surfaces were optically examined and photographed. The length and depths of the features on the fracture surfaces were measured to produce flaw profiles. Portions of the fracture surfaces were removed and cleaned with inhibited acid and a soft bristle brush. The cleaned fracture surfaces were examined in a scanning electron microscope (SEM) to document the fracture morphology and to determine if there was any evidence of in-service growth by fatigue. Axial cross-sections were removed from the mating fracture surfaces, mounted, polished, and etched. Light photomicrographs were taken to document the feature morphologies and steel microstructure.

Mechanical testing (duplicate tensiles and full Charpy curve) was performed on transverse and axial, base metal and seam weld samples removed from the failed pipe joint. Chemical analysis was performed on a steel sample removed from the failed pipe joint to determine the composition.

The results of the analysis indicate that the leak occurred at a colony of circumferentially oriented, OD surface breaking, interlinked near-neutral-pH stress corrosion cracks that were located near the longitudinal seam weld. The seam weld was located at the 2:00 o'clock orientation.

Supporting evidence for the conclusion that the cause of the rupture was near-neutral-pH SCC includes: (1) the presence of a colony of circumferentially oriented cracks on the external surface of the pipe in the vicinity of the failure origin; (2) the interlinking of individual thumbnail shaped cracks within the colony to form the initiating flaw; (3) the transgranular path of the cracks within the colony; (4) the presence of other crack colonies in the vicinity of the failure origin; and (5) evidence of corrosion of the crack faces. The stress corrosion cracks propagated nearly through wall, which lead to final failure by ductile overload. ID surface breaking mill formed cracks (chatter marks) that were present in the previous investigation of this line pipe were not present in the current investigation.

Below is a summary of our observations and conclusions:

- The leak occurred within a colony of OD surface breaking circumferentially oriented cracks.

- The maximum depth of the crack at the leak site was 4.8 mm (100% of nominal wall thickness) deep. The length of the crack that contained the leak was 69.85 mm long.
- Several other crack colonies were present on the pipe joint. All of the cracks in the colonies were circumferentially oriented.
- Most colonies were located between the 1:30 and 2:30 o'clock orientations. One colony was located at the 9:44 o'clock orientation.
- The cracks within the colonies were characteristic of near-neutral-pH stress corrosion cracks.
- There was no evidence of fatigue crack growth of the stress corrosion cracks.
- The base metal tensile properties and chemical composition of the joint that failed meet specifications for API 5L X42 line pipe steel at the time of construction.
- The tensile properties of the pipe were better in the axial direction than the transverse direction.
- The average yield strength (YS) and ultimate tensile strength (UTS) for the duplicate transverse base metal samples were 350 MPa and 477 MPa, respectively.
- The average YS and UTS for the duplicate axial base metal samples were 374 MPa and 493 MPa, respectively.
- The average UTS of duplicate transverse samples removed from the seam weld for the pipe section was 529 MPa.
- The average UTS of duplicate axial samples removed from the seam weld for the pipe section was 586 MPa.
- The upper shelf Charpy energies (full size) for the transverse base metal, axial base metal, transverse seam weld, and axial seam weld samples were 40 J, 89 J, 17 J, and 107 J, respectively.
- The 85% FATT temperatures (full size) for the transverse base metal, axial base metal, transverse seam weld, and axial seam weld samples were 9.3ºC, 15.6ºC, 110.7ºC, and -5.9 ºC, respectively.
- The microstructure of the pipe steel is consistent with the vintage and grade.

Several different regions were found on the fracture surfaces. Below is a summary of the regions:

- Region 1 (in all Colonies) – Transgranular, quasi-cleavage fracture (pre-existing, thumbnail shaped stress corrosion crack).
- Region 2 (in all Colonies) – Cleavage fracture from laboratory overload (brittle).
- Region 3 (in Colony 3) - Ductile fracture
  - Leak location, Colony 3 - Ductile fracture at the leak location, in-service.
- Region 4 (in Colony 3) – Mechanically damaged and corroded fracture surface near the ID surface.

Table of Contents

List of Tables

List of Tables (continued)

List of Figures

List of Figures (continued)

List of Figures (continued)

List of Figures (continued)

1.0 BACKGROUND

Pembina Pipeline Corporation (*Pembina*) retained Det Norske Veritas (U.S.A.), Inc. (*DNV*) to perform a metallurgical analysis on a section of pipe from the eight-inch nominal diameter Deer Mountain Lateral crude oil pipeline that leaked. The leak was discovered on August 15, 2011 near Swan Hills, Alberta at kilometer post (KP) 44.007, 12.98 m from the upstream girth weld.

The portion of the pipeline that was removed is comprised 219 mm diameter by 4.8 mm wall thickness, API 5L X42 line pipe steel that contains an electric resistance welded (ERW) longitudinal seam. The maximum operating pressure (MOP) is 8275 kPa, which corresponds to 65.5% of the specified minimum yield strength (SMYS). The normal operating pressure is 5500 kPa, which corresponds to 43.5% of SMYS.

The pipeline was installed in 1961 and was externally coated with polyethylene tape and a fiberglass outer wrap. The coating at the leak was reportedly in poor condition and contained liquid under the coating; the pH of a liquid sample was 8.5.

Following construction, a hydrostatic pressure test was performed. The pipeline has an impressed current cathodic protection (CP) system that was installed in 1961. Cathodic protection readings were taken on July 31, 2011 in the vicinity of the leak. Pipe to soil potentials were 1353 mV (on).

In the field, the coating was removed, the pipe was cleaned, and magnetic particle inspection (MPI) was performed in the vicinity of the leak location. A 3.93 m section of pipe that contained the leak was shipped to DNV for analysis. The objectives of the analysis were to determine the metallurgical cause of the failure and identify any contributing factors.

2.0 TECHNICAL APPROACH

The procedures used in the analysis were in accordance with industry-accepted standards. Five of the general standards governing terminology, specific metallographic procedures, mechanical testing, and chemical analysis used are as follows:

- ASTM E7, “Standard Terminology Relating to Metallography.”
- ASTM E3, “Standard Methods of Preparation of Metallographic Specimens.”
- ASTM E8, “Test Methods for Tension Testing of Metallic Materials.”
- ASTM E23, “Standard Test Methods for Notched Bar Impact Testing of Metallic Materials.”

- ASTM A751, "Standard Test Methods, Practices, and Terminology for Chemical Analysis of Steel Products."

The following steps were performed for this analysis. The pipe section was visually inspected and photographed. Wall thicknesses, diameters, and circumferences were measured on the pipe ends where coating was not present. Portions of the pipe that contained MPI indications were cleaned with a solvent. MPI was performed at these indications and the pipe was photographed.

Pipe samples that contained the indications (including the leak location) were removed from the pipe section, placed in liquid nitrogen, and hit with a hammer to reveal the fracture surfaces. The fracture surfaces were optically examined and photographed. The length and depths of the features on the fracture surfaces were measured to produce flaw profiles. Portions of the fracture surfaces were removed and cleaned with inhibited acid and a soft bristle brush. The cleaned fracture surfaces were examined in a scanning electron microscope (SEM) to document the fracture morphology and to determine if there was any evidence of in-service growth by fatigue. Axial cross-sections were removed from the mating fracture surfaces, mounted, polished, and etched; see Figure 1 for the locations where samples were removed. Light photomicrographs were taken to document the feature morphologies and steel microstructure.

Mechanical testing (duplicate tensiles and full Charpy curve) was performed on transverse and axial, base metal and seam weld samples removed from the failed pipe joint. Chemical analysis was performed on a steel sample removed from the failed pipe joint to determine the composition; see Figure 1 for the locations where samples were removed.

3.0 RESULTS

3.1 Optical Examination

Figure 2 is a photograph of the pipe section after unwrapping. The pipe section had been wrapped in clear plastic and duct tape for shipment (not pictured). The portion that leaked was also wrapped with duct tape. The pipe section was approximately 3.93 m (12.9 feet) long and contained a longitudinal seam weld near the 2:00 orientation. The pipe section contained a girth weld that was 2.15 m downstream (D/S) from the leak location. Top-dead-center (TDC) and flow direction were not marked on the pipe section. DNV used magnetic particle inspection (MPI) data from the field to estimate the TDC location and flow direction.

Figure 3 is a photograph of the external pipe surface showing the circumferential oriented crack colony at the leak location (Colony 3). Colony 3 was located 1.45 m from the upstream (U/S) reference end at 1:39 o'clock orientation; further discussion of the crack colonies is given in Section 3.2. The presence of white paint on the external pipe surface confirmed that MPI was performed in the field. It appeared MPI was performed on approximately one-third of the external pipe surface.

Circumferences, diameters, and wall thickness were measured at the U/S and downstream (D/S) pipe section ends. The diameters calculated from circumference measurements were 220 mm; see Table 1. The diameters were measured with a tape measure from the 3 to 9 o'clock and 12 to 6 o'clock orientations. The diameters at the ends were 220 mm, indicating no ovality. The diameter values are consistent with nominal 219 mm diameter pipe. The wall thickness was measured at the 12, 3, 6, and 9 o'clock orientations; see Table 2. The average wall thickness values for the U/S and D/S ends were 4.83 mm and 4.59 mm, respectively. These wall thickness values are consistent with the nominal wall thickness of 4.8 mm.

3.2 Magnetic Particle Inspection

Laboratory MPI of the external pipe surface was performed where crack colonies were identified in the field. Figure 4 through Figure 14 are optical photographs of the colonies following MPI of the external surface. Table 3 is a summary of the crack colony locations and dimensions. The first column in the table is the assigned crack colony identification number. Twelve crack colonies were identified during laboratory MPI. Crack Colony 3 contained the leak and MPI was not performed, at the request of the client. Crack Colony 8 and Crack Colony 9 consisted of two sub colonies. The second column in the table is the distance from the U/S reference end of the pipe to the U/S end of the colony. The third column is the o'clock orientation of the center of the colony. The fourth and fifth columns of the table are the axial and circumferential length of the colony, respectively.

3.3 Internal Surface

Figure 15 is a photograph of the internal pipe surface at the leak site, where Crack Colony 3 was located on the external pipe surface. The black dashed lines indicate the crack tips on the inside surface. The ID surface breaking portion of the crack is approximately 10 mm (0.49 inches) long. The figure shows some deformation around the crack. The seam weld is indicated in the figure. The seam weld is slightly raised in some locations, which indicates that the trimming process did not remove all of the excess weld metal.

3.4 Fractography

The fracture surfaces for Crack Colony 1 could not be broken open after several attempts. The crack flaw is assumed to be shallow in contrast to the remaining Crack Colonies. The remaining Crack Colonies were broke open without issue.

Figure 16 through Figure 25 are photographs of the fracture surface after breaking open cracks at Colony 2 through Colony 12. Two regions are identified on the fracture surfaces. Region 1 consists of a few to several, OD surface breaking, pre-existing thumbnail cracks with a black appearance. Region 2 consists of the remainder of the fracture surface and has a grey and shiny appearance. Region 2 is the overload region that occurred in the laboratory.

Detailed crack length and depth measurements of the previously described thumbnail cracks and axial feature were taken to generate flaw profiles; see Figure 27, Figure 28, and Figure 29 for the graphs and Table 4 through Table 14 for length and depths. Table 15 summarizes the maximum depth of each flaw profile (length vs. depth) for the pre-existing thumbnail shaped cracks located on the fracture surfaces removed from crack colonies. The maximum depth of the non-through wall crack colonies was less than 50 percent of the wall thickness. Figure 27 shows the flaws from the cracks and features removed from Colonies 2, 4, 5, 6, and 7. The figure shows that the thumbnail cracks for these colonies were less than 2.1 mm deep. Figure 27 shows the flaws from the cracks and features removed from Colonies 8, 9, 10, 11, and 12. The figure shows that the thumbnail cracks for these colonies were less than 1.9 mm deep. Crack Colony 2 and Crack Colony 6 were selected for further investigation because each contained cracks that penetrated over 40 percent of the wall thickness.

Figure 29 shows the flaw from the crack and features removed from Colony 3. The overall length of the crack was larger (69.85 mm) than recorded previously (55 mm). This is because MPI was not completed on this crack colony, thus the edges of the crack had not been clearly identified previously. Crack Colony 3 was through wall in two locations.

3.5 Scanning Electron Microscopy

Figure 30 is an SEM image of fracture surface Sample S1 from Colony 2. The dashed line in the figure separates the pre-existing thumbnail crack (Region 1) from the laboratory fracture region (Region 2). Figure 31 is a high magnification SEM image of the interface between Region 1 and 2. The fracture surface in Region 1 is corroded but contains some features consistent with quasi-cleavage. Quasi-cleavage is characteristic of near-neutral pH SCC. The figure also shows the cleavage facets that occurred in Region 2. The cleavage facets are consistent with brittle overload and formed during breaking open the sample in the laboratory. There was no evidence of fatigue striations near the interface between Region 1 and 2.

Figure 32 is an SEM image of fracture surface Sample S2 from Colony 3 (the leak location). The dashed line in the figure separates the pre-existing thumbnail crack (Region 1) from the overload regions (Region 3 and 4). Figure 33 is an SEM image near the ID surface of Sample S2. The figure shows a corroded surface in Region 1 above an overload region (Region 3 and Region 4). Figure 34 is a high magnification SEM image of Region 1 in the area indicated in Figure 32. The fracture surface in Region 1 is corroded but contains features consistent with quasi-cleavage. There also are a number of pits on the fracture surface in Region 1 that probably initiated at inclusions in the steel. Figure 35 is a SEM image in Region 3. The figures show a generally smeared morphology with some dimpled features. Dimples are consistent with ductile overload. This morphology was visible throughout Region 3. Dashed lines indicate the boundaries of Region 3. It is not obvious when Region 3 (ductile overload) at this location on the pipe

occurred. Figure 36 is a high magnification SEM image of the overload region adjacent to Region 3 (Region 4). The figure shows that Region 4 has been severely corroded and smeared. It is not obvious when this region overloaded; however, the damage to the fracture surface indicates that overload occurred prior to the laboratory investigation.

Figure 37 is an SEM image of fracture surface Sample S3 from Colony 6. The dashed line in the figure separates the pre-existing thumbnail crack (Region 1) from an overload region (Region 2). Pits are evident in Region 1 on this fracture surface as well. Figure 38 is an SEM image showing the interface of Region 1 and Region 2. The features in Region 1 are corroded but contain some features that are consistent with quasi-cleavage. The cleavage facets in Region 2 are consistent with brittle overload and formed during breaking open the sample in the laboratory. There was no evidence of fatigue striations near the interface between Region 1 and 2.

3.6 Metallography

Figure 39 is a stereo light photomicrograph of axial metallographic section (Mount M1) that was removed from Crack Colony 2. A relatively straight crack path is visible. Other than the crack that was broken open, no additional surface breaking features were present in the metallograhic section. Figure 40 is a close-up of the cross-section of the fracture surface of Mount 1 in Region 1; area indicated in Figure 39. The crack path appears to be transgranular.

Figure 41 is a stereo light photomicrograph of axial metallographic section (Mount M2) that was removed from Crack Colony 3 (leak location). No surface breaking features were present in the metallograhic section. Figure 42 is stereo light photomicrograph of the fracture surface in Region 1 near the ID surface. The figure shows secondary cracks branching off from the primary crack. The dashed line indicates the interface between Region 1 (pre-existing stress corrosion crack) and 3 (ductile overload). Figure 43 is a close-up light photomicrograph of Mount 2 near the ID surface. The transgranular secondary crack tip has been opened up due to ductile overload. Slight deformation of the metal at the ID surface is visible. Figure 44 is a light photomicrograph of the typical microstructure of the base metal. The microstructure consists of ferrite (white areas), pearlite (gray areas consisting of lamellae), and inclusions (dark areas). This microstructure is consistent with the vintage and grade of the steel.

Figure 45 is a stereo light photomicrograph of the axial metallographic section (Mount M3) that was removed from Crack Colony 6. A second OD surface breaking crack is visible. Figure 46 is a close-up light photomicrograph of the second crack tip. The figure shows that the crack path is transgranular, which is consistent with near neutral pH SCC. The primary crack path in Region 1 (Figure 45) is relatively straight in appearance. Figure 47 is a light photomicrograph of Mount M3 showing the cross-section of the fracture surface. The crack path appears to be transgranular and a secondary crack is visible.

3.7 Mechanical Testing

The results of the base metal and seam weld tensile testing are shown in Table 16. The average yield strength (YS) and ultimate tensile strength (UTS) for the duplicate transverse base metal samples were determined to be 350 MPa and 477 MPa, respectively. The average YS and UTS for the duplicate axial base metal samples were determined to be 374 MPa and 493 MPa, respectively. The YS and UTS values in both directions exceed the minimum YS and UTS specification for API 5L Grade X42 line pipe steel of 290 MPa, and 414 MPa, respectively, at the time of manufacture.

The average UTS of duplicate transverse samples removed from the seam weld for the pipe section was 529 MPa, which exceeds the minimum specified value for API 5L Grade X42 line pipe steel of 414 MPa. The average UTS of duplicate axial samples removed from the seam weld for the pipe section was 586 MPa, which exceeds the minimum specified value for API 5L Grade X42 line pipe steel of 414 MPa. YS values across the weld are not reliable and are not specified in API 5L.

Table 17 through Table 20 summarizes the results of the Charpy testing for the base metal and seam weld samples while Figure 48 through Figure 55 show the Charpy percent shear and impact energy curves. An analysis of the data for the axial base metal indicates that the 85% fracture appearance transition temperature (FATT) is -8.7°C and the upper shelf Charpy energy is 89 J, full size. An analysis of the data for the transverse base metal indicates that the 85% FATT is -14.9°C and the upper shelf Charpy energy is 40 J, full size. An analysis of the data for the axial seam weld indicates that the 85% FATT is -30.3°C and the upper shelf Charpy energy is 107 J, full size. An analysis of the data for the transverse seam weld indicates that the 85% FATT is 86.3°C and the upper shelf Charpy energy is 17 J, full size.

The CVN test results can be adjusted to account for material constraint effects by applying temperature shifts to the data.[1] The full size transition temperatures (brittle-to-ductile fracture initiation temperature) for the axial base metal, transverse base metal, axial seam weld, and transverse seam weld samples were 15.6°C, 9.3°C, -5.9°C, and 110.7°C, respectively, based on a nominal pipe wall thickness of 4.8 mm; see Table 21. The tested materials are expected to exhibit ductile fracture behavior above their full size transition temperatures.

3.8 Chemical Analysis

The results of the chemical analysis performed on a sample removed from the pipe joint that leaked are shown in Table 22. The results show that the pipe joint meets composition specifications for API 5L Grade X42 line pipe steel at the time of manufacture.

1 "A Simple *Procedure* for Synthesizing Charpy Impact Energy Transition Curves from Limited Test Data," Michael J. Rosenfeld, International Pipeline Conference – Volume 1, ASME 1996, p. 216.

4.0 CONCLUSIONS

The results of the analysis indicate that the leak occurred at a colony of circumferentially oriented, OD surface breaking, interlinked near-neutral-pH stress corrosion cracks that were located near the longitudinal seam weld. The seam weld was located at the 2:00 o'clock orientation.

Supporting evidence for the conclusion that the cause of the rupture was near-neutral-pH SCC includes: (1) the presence of a colony of circumferentially oriented cracks on the external surface of the pipe in the vicinity of the failure origin; (2) the interlinking of individual thumbnail shaped cracks within the colony to form the initiating flaw; (3) the transgranular path of the cracks within the colony; (4) the presence of other crack colonies in the vicinity of the failure origin; and (5) evidence of corrosion of the crack faces. The stress corrosion cracks propagated nearly through wall, which lead to final failure by ductile overload. ID surface breaking mill formed cracks (chatter marks) that were present in the previous investigation of this line pipe were not present in the current investigation.

Below is a summary of our observations and conclusions:

- The leak occurred within a colony of OD surface breaking circumferentially oriented cracks.
- The maximum depth of the crack at the leak site was 4.8 mm (100% of nominal wall thickness) deep. The length of the crack that contained the leak was 69.85 mm long.
- Several other crack colonies were present on the pipe joint. All of the cracks in the colonies were circumferentially oriented.
- Most colonies were located between the 1:30 and 2:30 o'clock orientations. One colony was located at the 9:44 o'clock orientation.
- The cracks within the colonies were characteristic of near-neutral-pH stress corrosion cracks.
- There was no evidence of fatigue crack growth of the stress corrosion cracks.
- The base metal tensile properties and chemical composition of the joint that failed meet specifications for API 5L X42 line pipe steel at the time of construction.
- The tensile properties of the pipe were better in the axial direction than the transverse direction.

- The average yield strength (YS) and ultimate tensile strength (UTS) for the duplicate transverse base metal samples were 350 MPa and 477 MPa, respectively.
- The average YS and UTS for the duplicate axial base metal samples were 374 MPa and 493 MPa, respectively.
- The average UTS of duplicate transverse samples removed from the seam weld for the pipe section was 529 MPa.
- The average UTS of duplicate axial samples removed from the seam weld for the pipe section was 586 MPa.
- The upper shelf Charpy energies (full size) for the transverse base metal, axial base metal, transverse seam weld, and axial seam weld samples were 40 J, 89 J, 17 J, and 107 J, respectively.
- The 85% FATT temperatures (full size) for the transverse base metal, axial base metal, transverse seam weld, and axial seam weld samples were 9.3ºC, 15.6ºC, 110.7ºC, and -5.9 ºC, respectively.
- The microstructure of the pipe steel is consistent with the vintage and grade.

Several different regions were found on the fracture surfaces. Below is a summary of the regions:

- Region 1 (in all Colonies) – Transgranular, quasi-cleavage fracture (pre-existing, thumbnail shaped stress corrosion crack).
- Region 2 (in all Colonies) – Cleavage fracture from laboratory overload (brittle).
- Region 3 (in Colony 3) - Ductile fracture
  - Leak location, Colony 3 - Ductile fracture at the leak location, in-service.
- Region 4 (in Colony 3) – Mechanically damaged and corroded fracture surface near the ID surface.

Table 1. Results of circumference and diameter measurements performed on the U/S and D/S ends of the pipe section.

Pipe Section End	Circumference (mm)	Diameter from Circumference Measurement (mm)	Diameter 3 to 9 o'clock (mm)	Diameter 6 to 12 o'clock (mm)
U/S	691	220	220	220
D/S	691	220	220	220

Table 2. Results of wall thickness measurements performed on the U/S and D/S ends of the pipe section.

O'clock Orientations	Wall Thickness, U/S End (mm)	Wall Thickness, D/S End (mm)
12:00	4.83	4.60
3:00	4.83	4.57
6:00	4.83	4.60
9:00	4.83	4.60
Average	4.83	4.59

Table 3. Summary of crack colony locations.

Crack Colony	Distances from Reference End (m)[1]	O'clock Orientation[4]	Axial Length (mm)	Circumferential Length (mm)
1	0.645	9:44	1	3
2	0.840	1:44	1	7
3	1.450	1:39	9	55
4	1.795	2:44	25	35
5	1.939	2:44	12	40
6	1.972	2:44	13	35
7	2.185	2:00	5	5
8A	2.319[2]	2:00	7	22
8B	2.325[2]	2:00	4	15
9A	2.347[3]	2:00	2	7
9B	2.352[3]	2:00	14	11
10	2.378	2:00	11	20
11	0.883	2:05	29	25
12	1.034	2:21	1	6

1. Distance from U/S reference end to the U/S end of the colony.
2. Sub colonies of Crack Colony 8.
3. Sub colonies of Crack Colony 9.
4. Measured to the center of the colony.

Table 4. Flaw profile (length vs. depth) for the pre-existing thumbnail shaped crack located on the fracture surface removed from Crack Colony 2.

Length (mm)	Depth	
	mm	% of nominal wall thickness
0.00	0.00	0.0
1.59	1.96	40.7
3.18	1.91	39.7
4.76	1.60	33.3
6.35	0.46	9.5
7.94	0.00	0.0

Table 5. Flaw profile (length vs. depth) for the pre-existing thumbnail shaped crack located on the fracture surface removed from Crack Colony 3.

Length (mm)	Depth	
	mm	% of nominal wall thickness
0.00	0.00	0.0
1.59	0.71	14.8
3.18	1.68	34.9
4.76	1.96	40.7
6.35	2.13	44.5
7.94	2.21	46.0
25.40	2.74	57.2
26.99	3.15	65.6
28.58	3.18	66.1
30.16	3.25	67.7
31.75	3.20	66.7
33.34	3.45	72.0
50.80	3.86	80.4
52.39	4.17	86.8
53.98	4.01	83.6
55.56	4.80	100.0
57.15	4.80	100.0
58.74	4.80	100.0
60.33	4.09	85.2
61.91	3.23	67.2
62.67	3.53	73.6
64.26	3.66	76.2
65.85	3.78	78.8
67.44	2.90	60.3
69.02	4.60	95.8
70.61	4.80	100.0
72.20	4.80	100.0
73.79	4.80	100.0
75.37	4.80	100.0
76.96	1.45	30.2
78.55	2.64	55.0
80.14	3.02	63.0
81.72	2.79	58.2
83.31	2.08	43.4
84.90	1.47	30.7
86.49	1.27	26.5
88.07	0.91	19.1
89.66	0.84	17.5
91.25	0.79	16.4
92.84	0.79	16.4
94.42	0.89	18.5
96.01	0.48	10.1
97.60	0.58	12.2
99.19	0.58	12.2
100.77	0.00	0.0

Table 6. Flaw profile (length vs. depth) for the pre-existing thumbnail shaped crack located on the fracture surface removed from Crack Colony 4.

Length (mm)	Depth	
	mm	% of nominal wall thickness
0.00	0.00	0.0
0.79	0.64	13.2
1.59	0.00	0.0
2.38	0.53	11.1
3.18	1.22	25.4
3.97	0.00	0.0
4.76	0.00	0.0
5.56	1.85	38.6
6.35	2.01	41.8
7.14	0.81	16.9
7.94	0.00	0.0
8.73	0.79	16.4
9.53	1.19	24.9
10.32	1.35	28.0
11.11	1.24	25.9
11.91	0.94	19.6
12.70	0.00	0.0

Table 7. Flaw profile (length vs. depth) for the pre-existing thumbnail shaped crack located on the fracture surface removed from Crack Colony 5.

Length (mm)	Depth	
	mm	% of nominal wall thickness
0.00	0.00	0.0
0.79	0.25	5.3
1.59	0.46	9.5
2.38	0.56	11.6
3.18	0.00	0.0

Table 8. Flaw profile (length vs. depth) for the pre-existing thumbnail shaped crack located on the fracture surface removed from Crack Colony 6.

Length (mm)	Depth	
	mm	% of nominal wall thickness
0.00	0.00	0.0
1.59	1.42	29.6
3.18	1.80	37.6
4.76	2.11	43.9
6.35	2.39	49.7
7.94	2.16	45.0
9.53	2.06	42.9
11.11	1.40	29.1
12.70	0.28	5.8
14.29	0.00	0.0
15.08	0.58	12.2
15.88	0.00	0.0
17.46	0.66	13.8
19.05	0.00	0.0
20.64	0.00	0.0
22.23	0.28	5.8
23.81	0.00	0.0

Table 9. Flaw profile (length vs. depth) for the pre-existing thumbnail shaped crack located on the fracture surface removed from Crack Colony 7.

Length (mm)	Depth	
	mm	% of nominal wall thickness
0.00	0.00	0.0
1.59	0.89	18.5
3.18	1.50	31.2
4.76	1.02	21.2
6.35	0.00	0.0

Table 10. Flaw profile (length vs. depth) for the pre-existing thumbnail shaped crack located on the fracture surface removed from Crack Colony 8A.

Length (mm)	Depth	
	mm	% of nominal wall thickness
0.00	0.00	0.0
1.59	0.46	9.5
3.18	0.00	0.0
4.76	0.69	14.3
5.56	0.00	0.0
6.35	0.33	6.9
7.14	0.69	14.3
7.94	0.00	0.0
8.73	0.28	5.8
9.53	1.12	23.3
11.11	1.65	34.4
12.70	1.24	25.9
14.29	1.30	27.0
15.88	1.78	37.0
17.46	1.63	33.9
19.05	1.85	38.6
20.64	1.60	33.3
22.23	1.47	30.7
23.81	1.09	22.8
25.40	0.58	12.2
26.19	0.00	0.0

Table 11. Flaw profile (length vs. depth) for the pre-existing thumbnail shaped crack located on the fracture surface removed from Crack Colony 9B.

Length (mm)	Depth	
	mm	% of nominal wall thickness
0.00	0.00	0.0
1.59	1.04	21.7
3.18	1.09	22.8
4.76	0.00	0.0

Table 12. Flaw profile (length vs. depth) for the pre-existing thumbnail shaped crack located on the fracture surface removed from Crack Colony 10.

Length (mm)	Depth	
	mm	% of nominal wall thickness
0.00	0.00	0.0
1.59	0.51	10.6
3.18	0.00	0.0
4.76	0.66	13.8
6.35	1.02	21.2
7.94	1.78	37.0
9.53	1.65	34.4
11.11	1.12	23.3
12.70	0.79	16.4
14.29	0.30	6.4
15.88	0.00	0.0

Table 13. Flaw profile (length vs. depth) for the pre-existing thumbnail shaped crack located on the fracture surface removed from Crack Colony 11.

Length (mm)	Depth	
	mm	% of nominal wall thickness
0.00	0.00	0.0
1.59	0.94	19.6
3.18	1.40	29.1
4.76	1.73	36.0
6.35	1.73	36.0
7.94	1.32	27.5
9.53	0.74	15.3
11.11	0.00	0.0

Table 14. Flaw profile (length vs. depth) for the pre-existing thumbnail shaped crack located on the fracture surface removed from Crack Colony 12.

Length (mm)	Depth	
	mm	% of nominal wall thickness
0.00	0.00	0.0
1.59	0.74	15.3
3.18	1.12	23.3
4.76	0.97	20.1
6.35	0.51	10.6
7.94	0.33	6.9
9.53	0.00	0.0

Table 15. Summary of the maximum depth of each flaw profile (length vs. depth) for the pre-existing thumbnail shaped cracks located on the fracture surfaces removed from crack colonies.

Crack Colony	Length (mm)	Depth	
		mm	% of nominal wall thickness
2	1.59	1.96	40.7
3	Through Wall Crack		
4	6.35	2.01	41.8
5	2.38	0.56	11.6
6	6.35	2.39	49.7
7	3.18	1.50	31.2
8	19.05	1.85	38.6
9	3.18	1.09	22.8
10	7.94	1.78	37.0
11	4.76	1.73	36.0
12	3.18	1.12	23.3

Table 16. Results of base metal and seam weld tensile tests performed on transverse and axial samples from the failed joint compared with specifications for API 5L Grade X42 line pipe steel.

	Transverse Base Metal	Axial Base Metal	Transverse Seam Weld	Axial Seam Weld	API 5L Grade X42 (Minimum Values) [2]
Yield Strength, MPa [1]	350	374	–	-	290
Tensile Strength, MPa [1]	477	493	529	586	414
Elongation in 2 inches, %	31.5	30.5	–	-	20.0
Reduction of Area, % [1]	44.0	51.0	–	-	–

1 – Average of duplicate tests.

2 – API Spec 5LX, 9th Edition, February 1960.

Table 17. Results of Charpy V-notch impact tests for transverse base metal samples removed from the failed pipe joint.

Sample ID	Temperature, °C	Sub-Size Impact Energy, J	Full Size Impact Energy, J	Shear, %	Lateral Expansion, mm
1	-51	2.7	6.6	0	0
2	-37	3.4	8.3	0	1
3	-26	4.7	11.5	5	4
4	-9	7.5	18.2	30	4
5	-4	10.8	26.2	85	10
6	4	14.2	34.4	90	15
7	18	16.3	39.3	95	18
8	32	15.6	38.0	98	17
9	46	17.6	42.6	100	18
10	60	16.3	39.0	100	13

Table 18. Results of Charpy V-notch impact tests for axial base metal samples removed from the failed pipe joint.

Sample ID	Temperature, °C	Sub-Size Impact Energy, J	Full Size Impact Energy, J	Shear, %	Lateral Expansion, mm
1	-101	0.7	1.8	0	0
2	-87	0.7	1.8	0	0
3	-65	1.4	3.7	0	1
4	-51	8.8	23.7	10	8
5	-37	14.9	40.5	30	16
6	-23	21.7	59.0	60	24
7	-9	27.1	73.2	80	32
8	4	31.2	84.7	100	43
9	18	32.5	87.9	100	41
10	38	31.9	86.6	100	45

Table 19. Results of Charpy V-notch impact tests for transverse seam weld samples removed from the failed pipe joint.

Sample ID	Temperature, °C	Sub-Size Impact Energy, J	Full Size Impact Energy, J	Shear, %	Lateral Expansion, mm
1	4	1.4	3.3	0	0
2	18	2.7	6.6	10	0
3	32	2.7	6.6	0	0
4	41	4.1	9.9	20	1
5	46	4.1	9.9	15	1
6	60	4.1	9.9	20	1
7	74	8.1	19.9	80	3
8	88	6.8	16.5	80	2
9	93	5.4	13.3	90	2
10	107	6.8	16.5	95	3

Table 20. Results of Charpy V-notch impact tests for axial seam weld samples removed from the failed pipe joint.

Sample ID	Temperature, °C	Sub-Size Impact Energy, J	Full Size Impact Energy, J	Shear, %	Lateral Expansion, mm
1	-129	2.0	5.7	0	0
2	-101	9.5	25.2	0	3
3	-73	14.9	40.3	25	14
4	-57	19.0	49.5	40	22
5	-48	21.7	60.6	55	22
6	-34	24.4	68.2	80	28
7	-21	32.5	87.9	100	34
8	-7	32.5	87.9	100	39
9	7	33.2	92.9	100	41
10	21	37.3	96.7	100	33

Table 21. Results of analysis of the Charpy V-notch impact energy and percent shear plots for base metal and seam weld samples removed from the failed pipe joint.

	Axial Base Metal	Transverse Base Metal	Axial Seam Weld	Transverse Seam Weld
Upper Shelf Impact Energy (Full Size), J	89	40	107	17
85% FATT, °C	-8.7	-14.9	-30.3	86.3
85% FATT, °C (Full Size)	15.6	9.3	-5.9	110.7

Table 22. Results of chemical analysis of a sample removed from the failed pipe joint compared with composition specifications (ladle analysis) for API 5L X42 line pipe steel.

Element		Composition (Wt. %)	API 5L X42 Spec (Wt. %) [1]
C	(Carbon)	0.221	0.28 (max)
Mn	(Manganese)	0.768	1.25 (max)
P	(Phosphorus)	0.009	0.04 (max)
S	(Sulfur)	0.025	0.05 (max)
Si	(Silicon)	0.107	–
Cu	(Copper)	0.134	–
Sn	(Tin)	0.021	–
Ni	(Nickel)	0.034	–
Cr	(Chromium)	0.031	–
Mo	(Molybdenum)	0.004	–
Al	(Aluminum)	0.001	–
V	(Vanadium)	0.000	–
Nb	(Niobium)	0.001	–
Zr	(Zirconium)	0.000	–
Ti	(Titanium)	0.001	-
B	(Boron)	0.0001	–
Ca	(Calcium)	0.0000	–
Co	(Cobalt)	0.005	–
Fe	(Iron)	Balance	Balance

1 – API Spec 5LX, 9th Edition, February 1960, welded, electric-furnace, open-hearth, basic-oxygen or killed deoxidized basic Bessemer, cold-expanded.

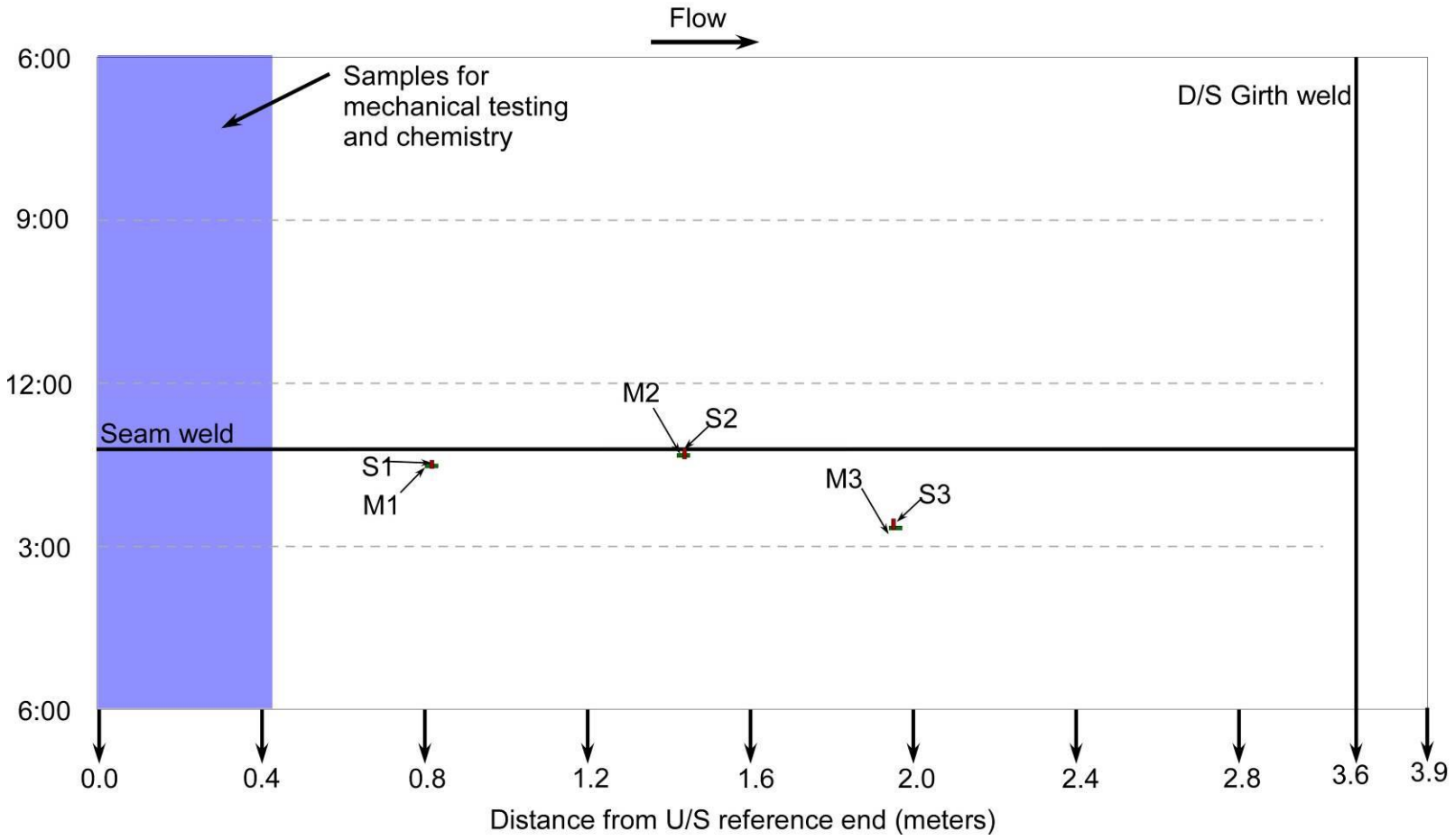

Figure 1. Schematic of pipe section showing the location of the seam weld and the locations where samples were removed for metallography (M1, 2, 3), fractography (S1, 2, 3), mechanical testing, and chemistry.

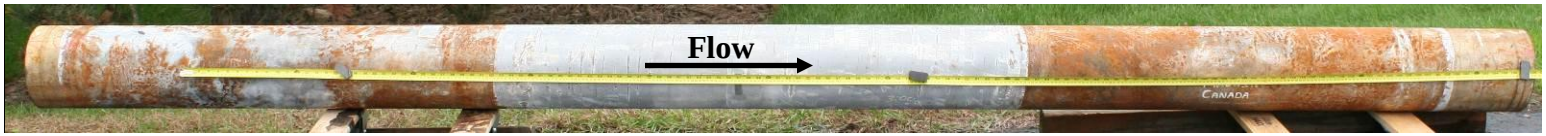

Figure 2. Photograph of the pipe section after unwrapping.

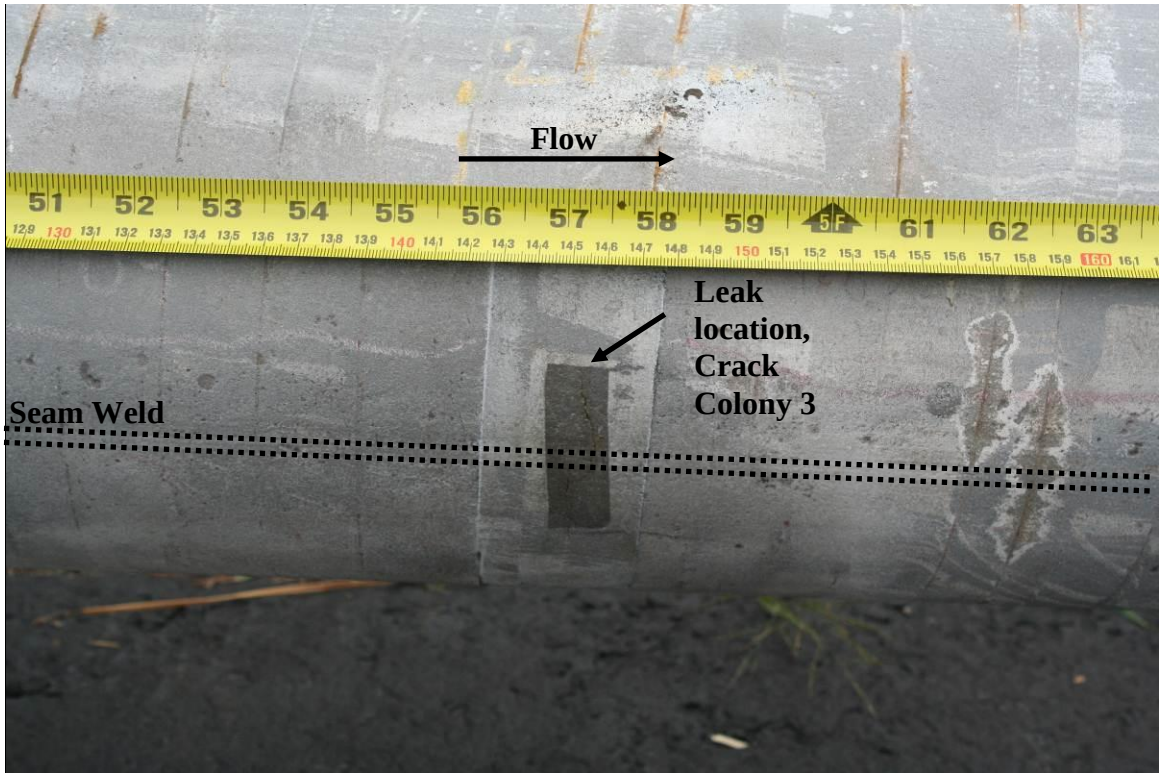

Figure 3. Photograph of the external pipe surface (prior to laboratory MPI) showing the leak location and crack colony. The tape measure indicates the distance from the U/S reference end.

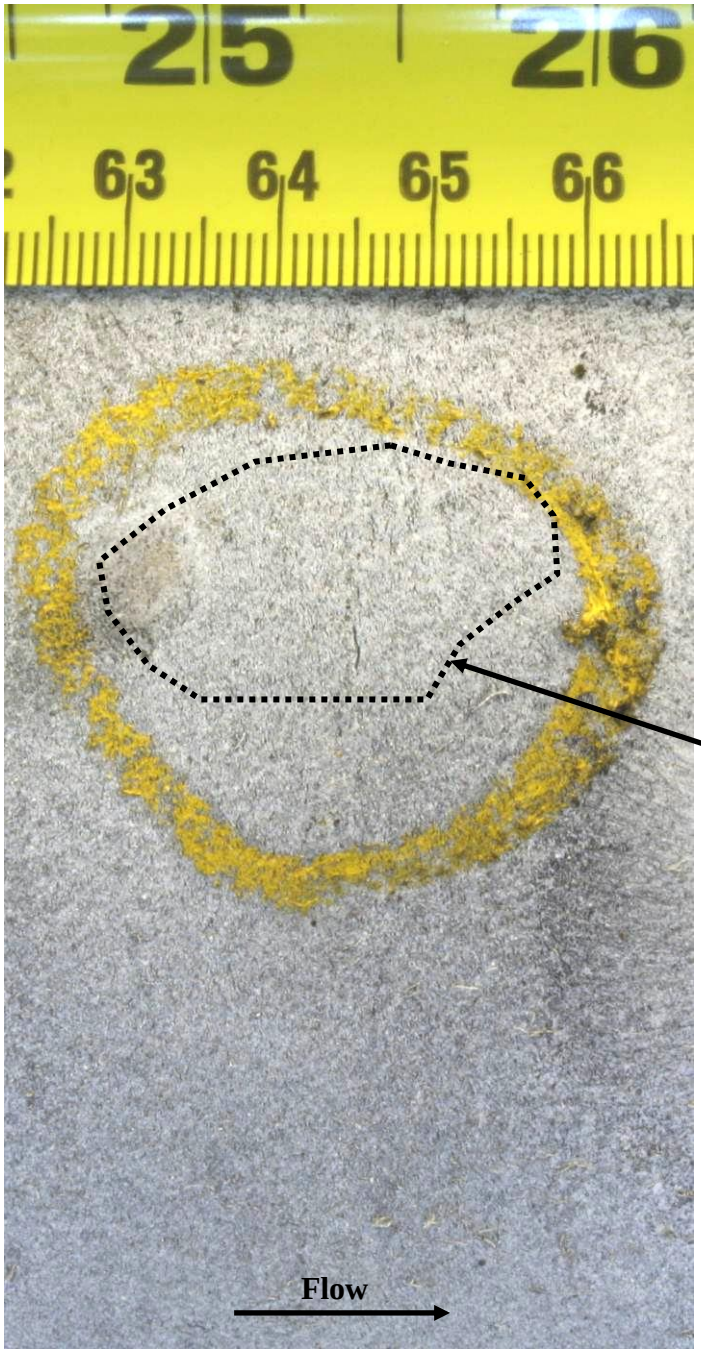

Figure 4. Photograph of the external pipe surface showing Crack Colony 1 following MPI. The tape measure indicates the distance from the U/S reference end.

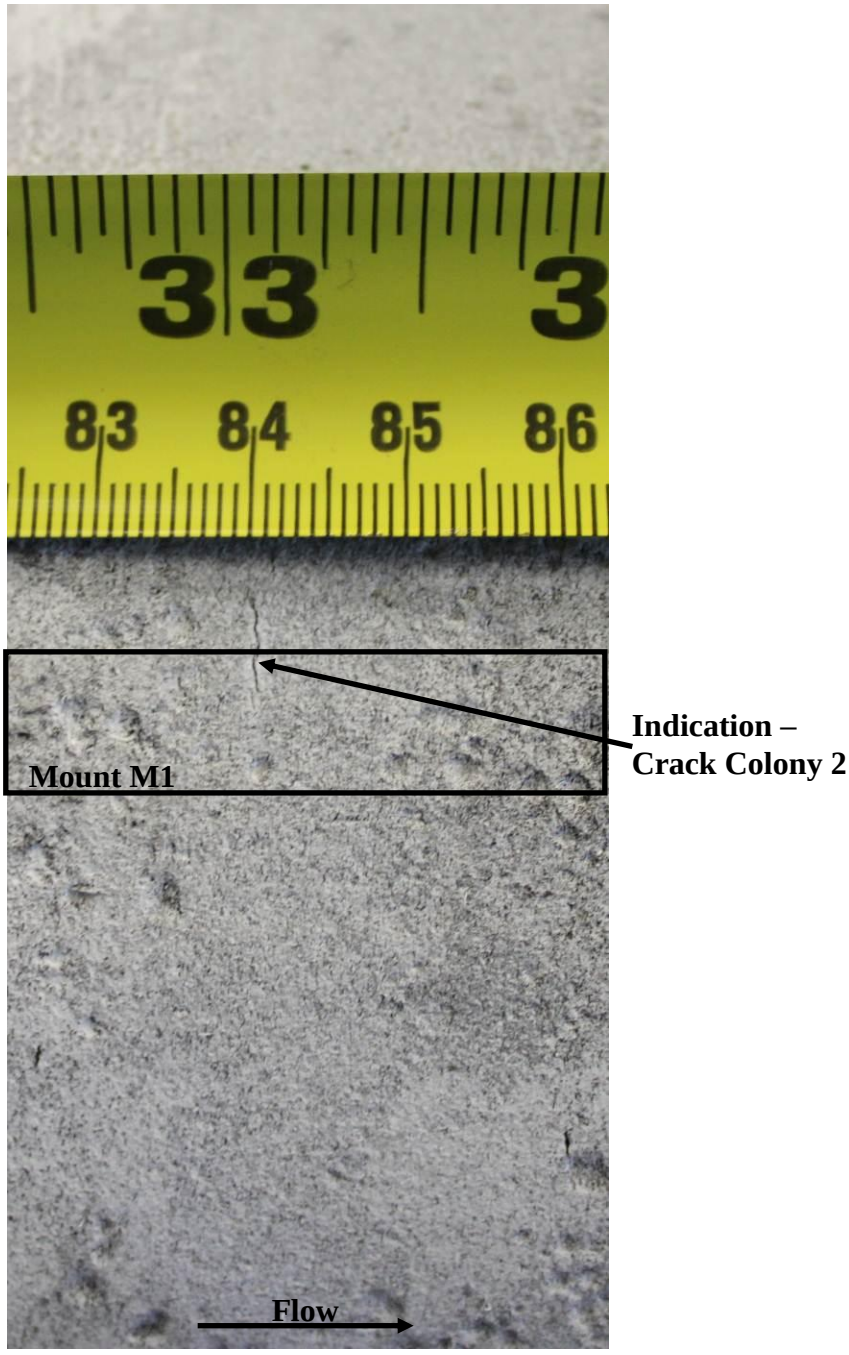

Figure 5. Photograph of the external pipe surface showing Crack Colony 2 following MPI. The tape measure indicates the distance from the U/S reference end.

Figure 6. Photograph of the external pipe surface showing Crack Colony 3 (Note: MPI was not performed in this area). The tape measure indicates the distance from the U/S reference end.

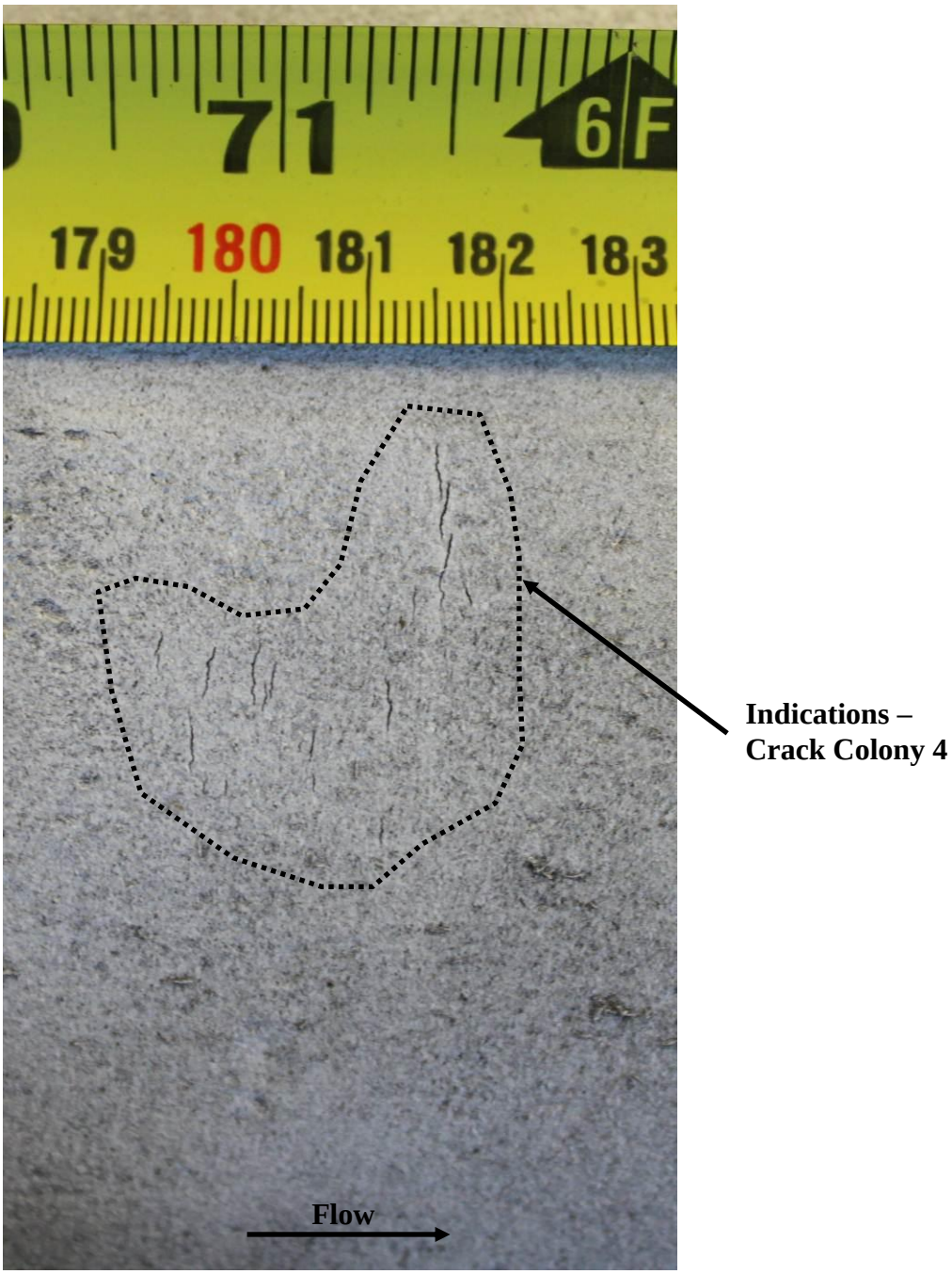

Figure 7. Photograph of the external pipe surface showing Crack Colony 4 following MPI. The tape measure indicates the distance from the U/S reference end.

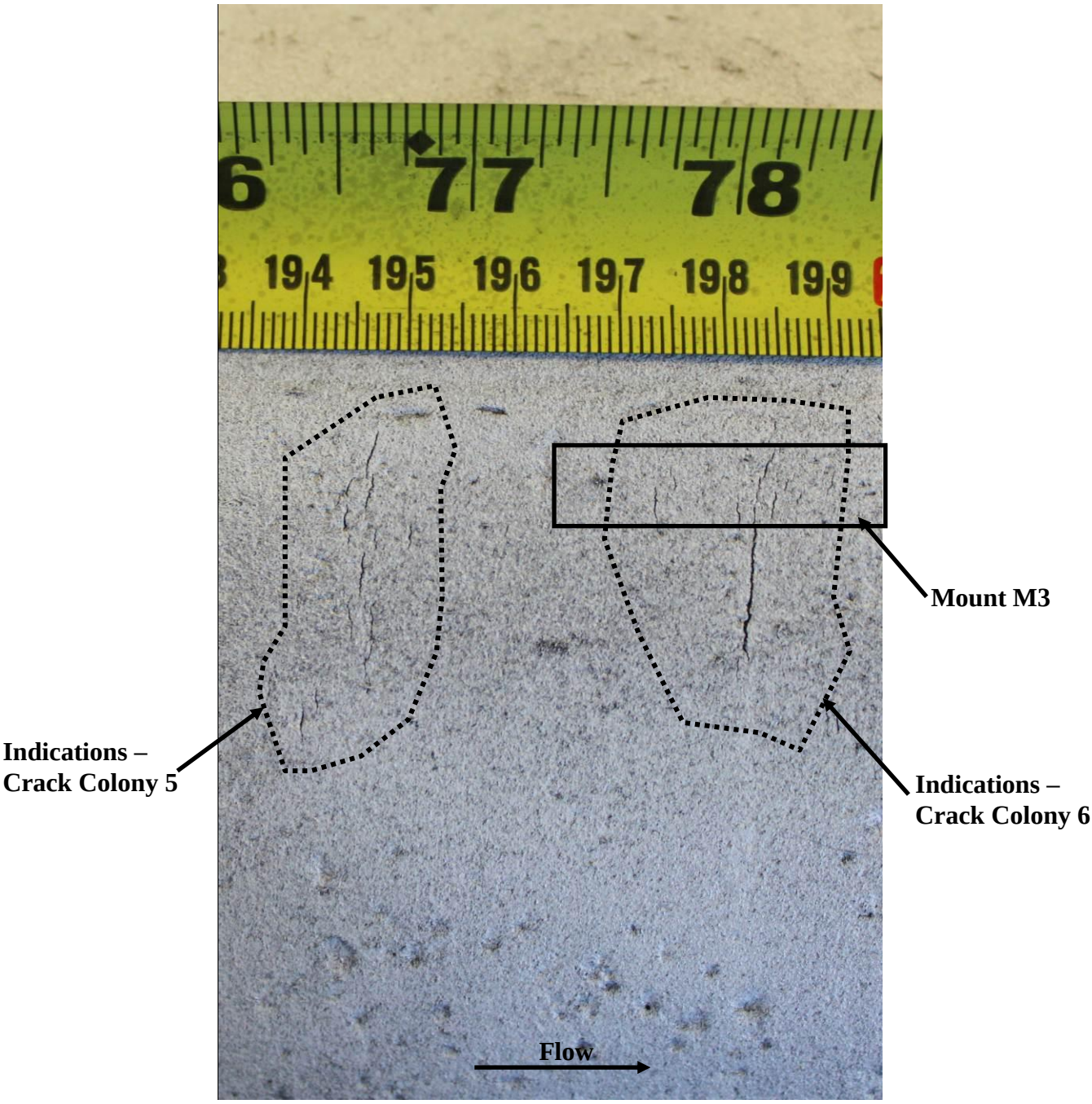

Figure 8. Photograph of the external pipe surface showing Crack Colony 5 and Crack Colony 6, following MPI. The tape measure indicates the distance from the U/S reference end.

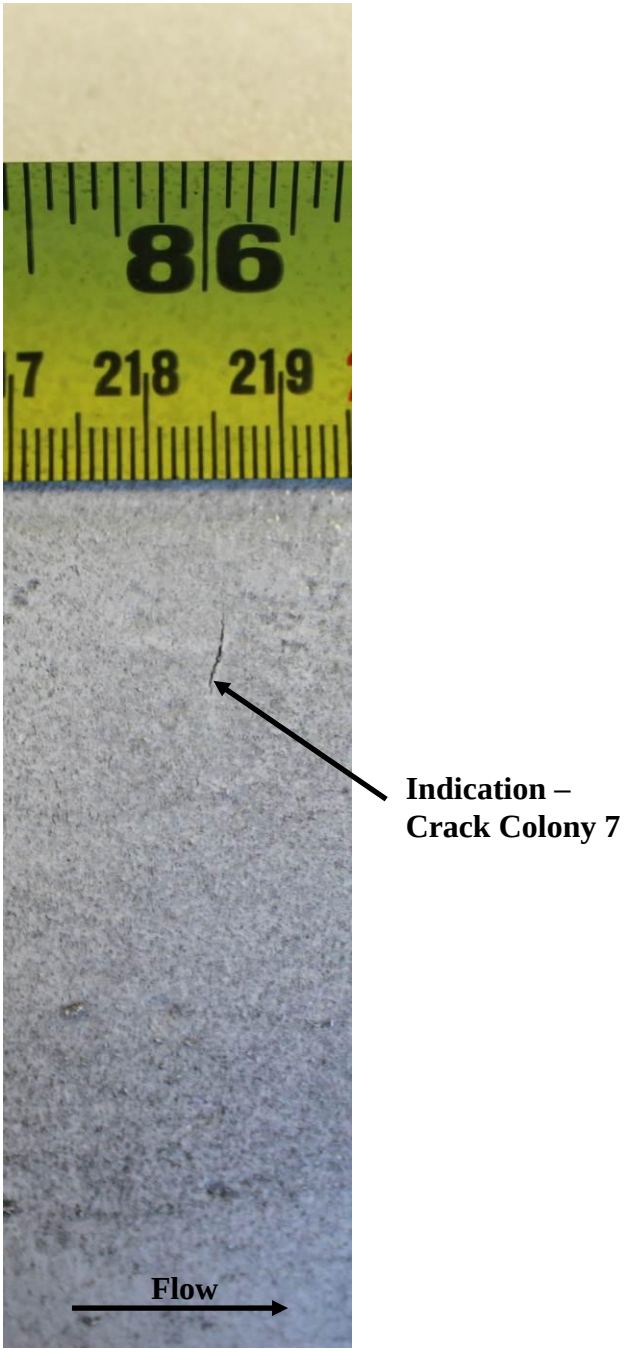

Figure 9. Photograph of the external pipe surface showing Crack Colony 7, following MPI. The tape measure indicates the distance from the U/S reference end.

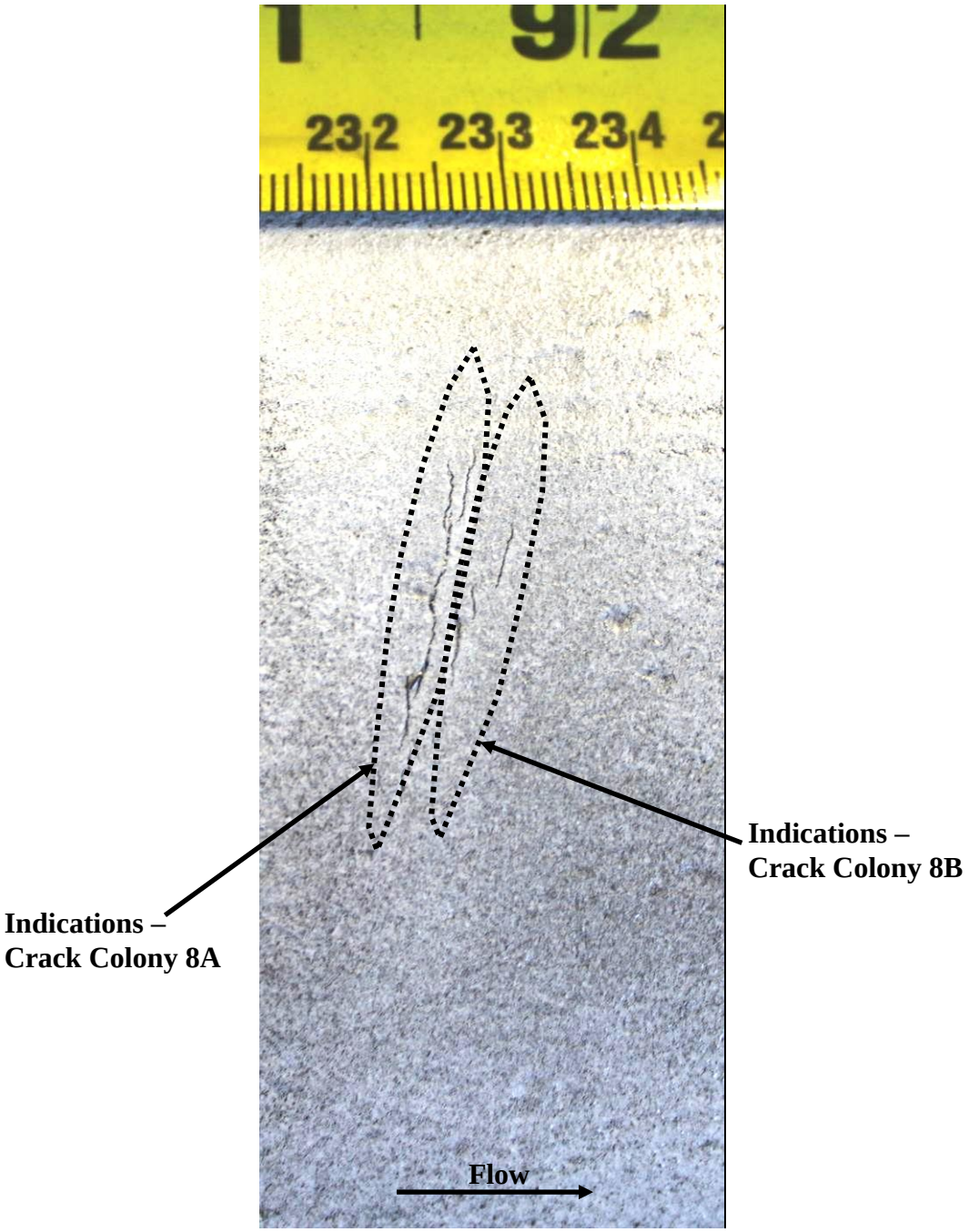

Figure 10. Photograph of the external pipe surface showing Crack Colony 8A and Crack Colony 8B, following MPI. The tape measure indicates the distance from the U/S reference end.

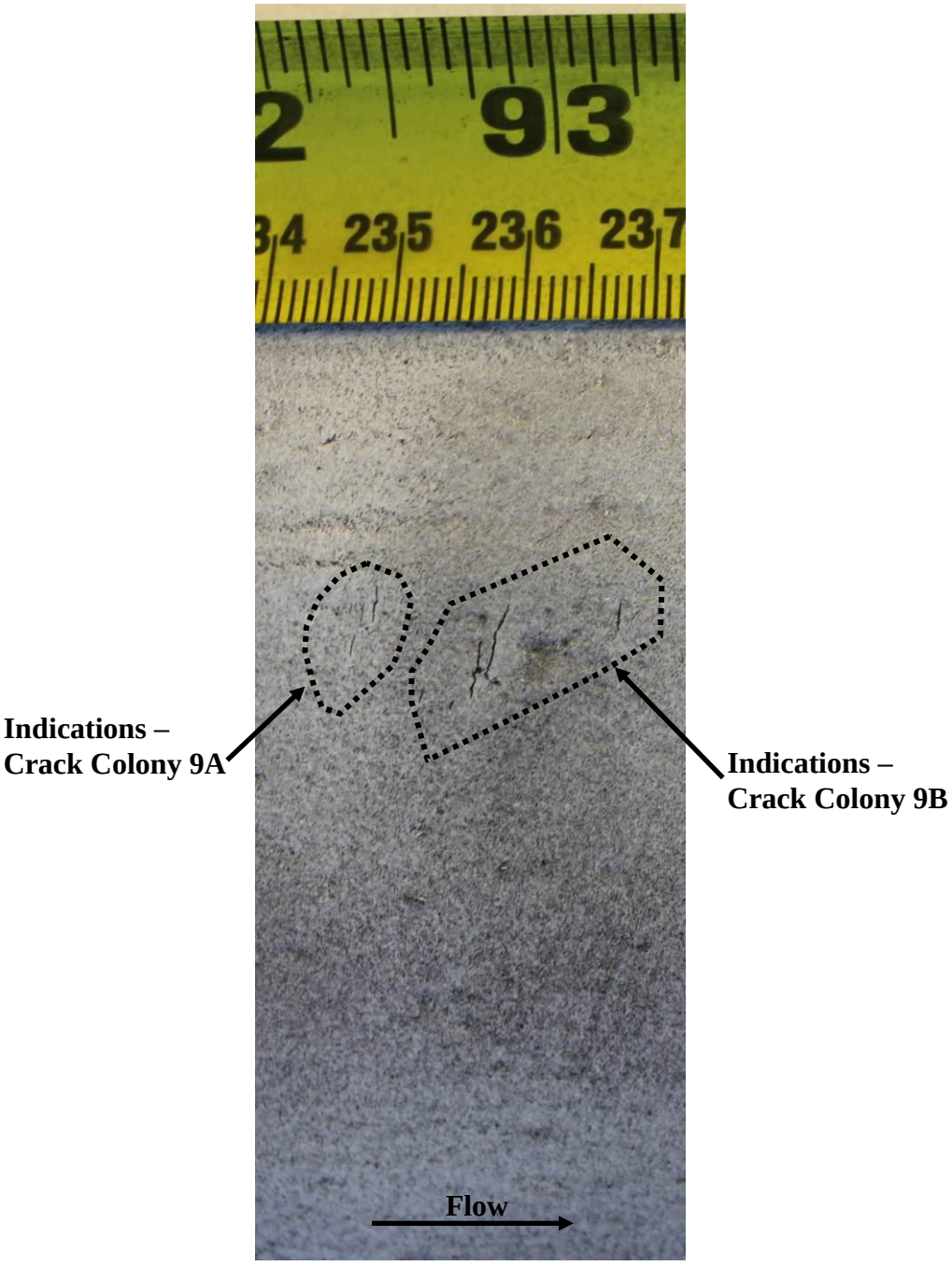

Figure 11. Photograph of the external pipe surface showing Crack Colony 9A and Crack Colony 9B, following MPI. The tape measure indicates the distance from the U/S reference end.

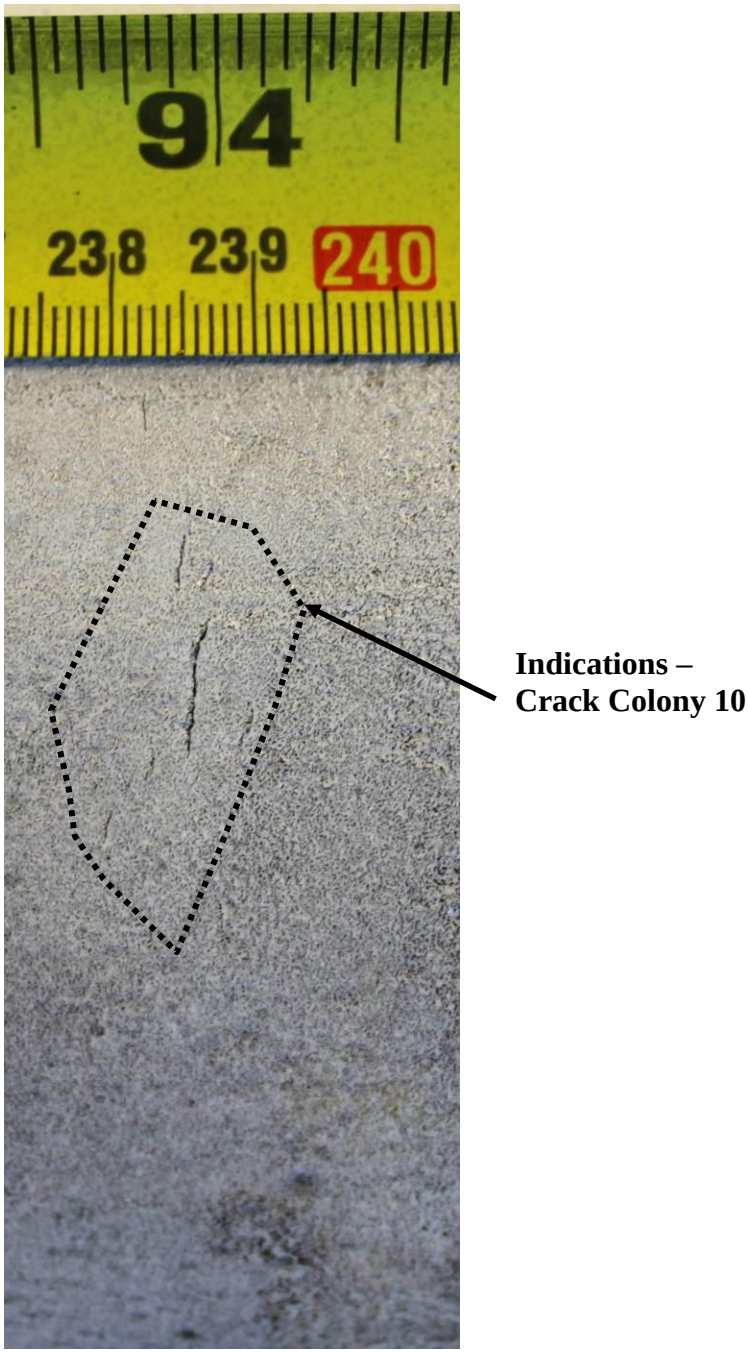

Figure 12. Photograph of the external pipe surface showing Crack Colony 10, following MPI. The tape measure indicates the distance from the U/S reference end.

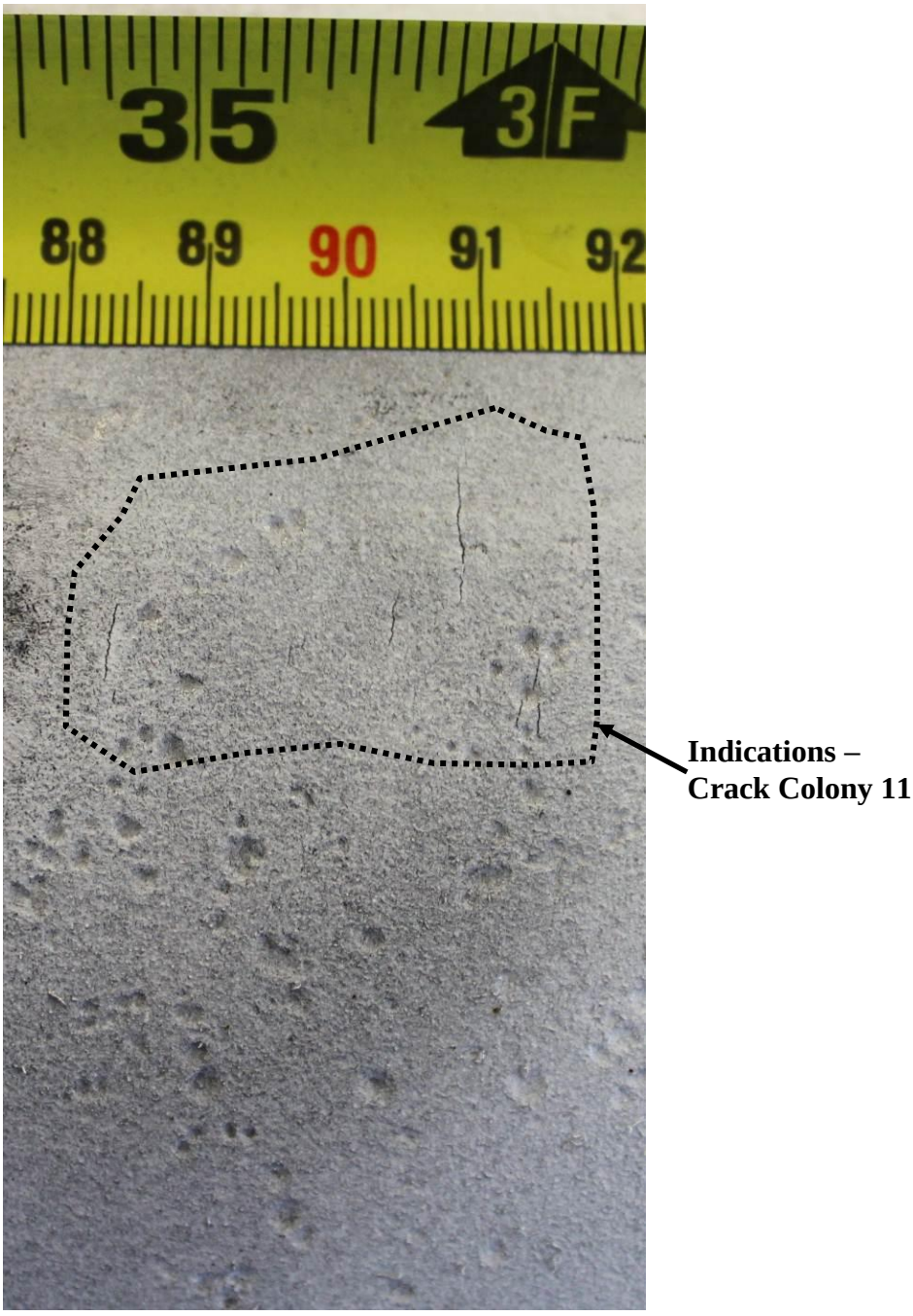

Figure 13. Photograph of the external pipe surface showing Crack Colony 11, following MPI. The tape measure indicates the distance from the U/S reference end.

Figure 14. Photograph of the external pipe surface showing Crack Colony 12, following MPI. The tape measure indicates the distance from the U/S reference end.

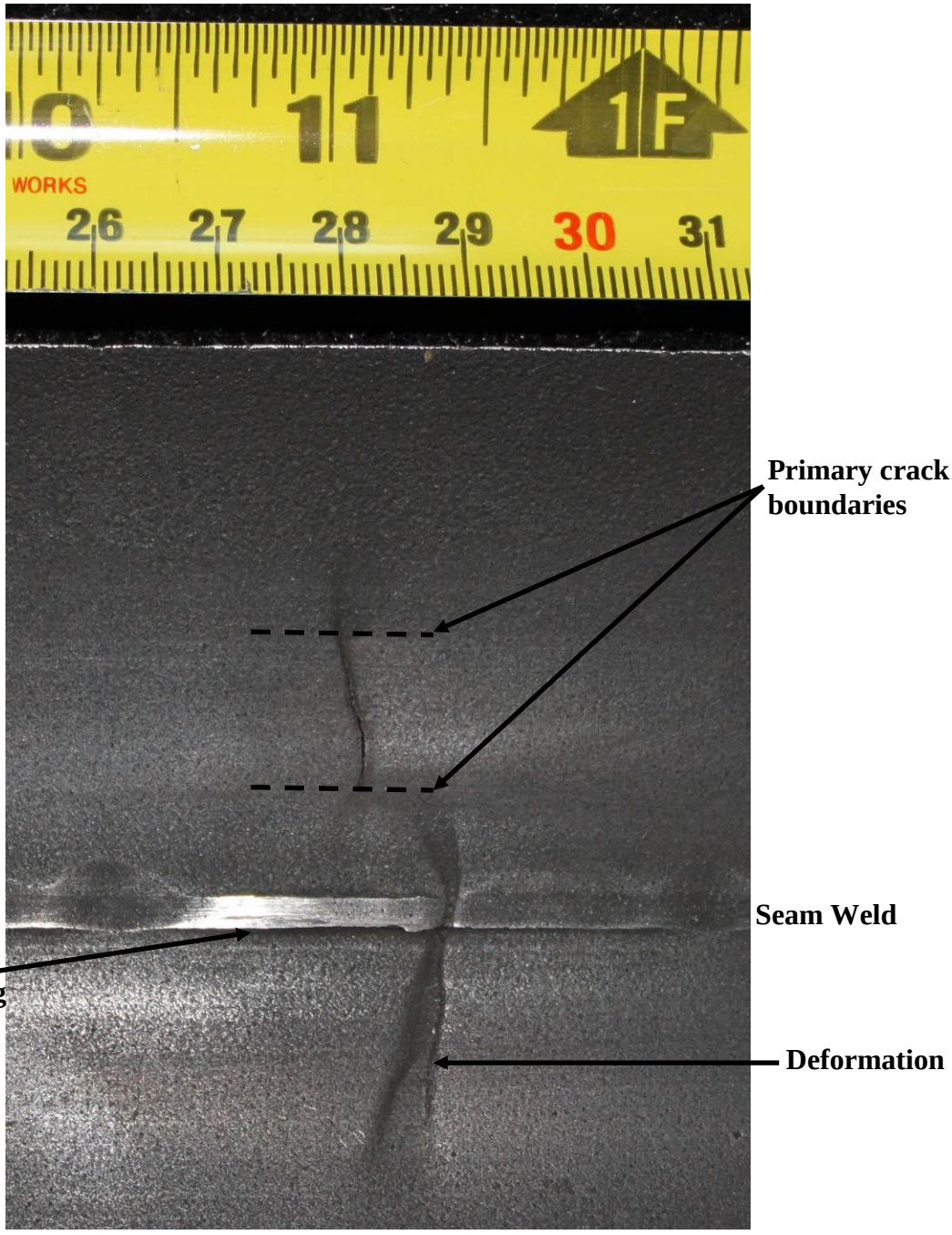

Figure 15. Photograph of the internal pipe surface at the leak location (Crack Colony 3).

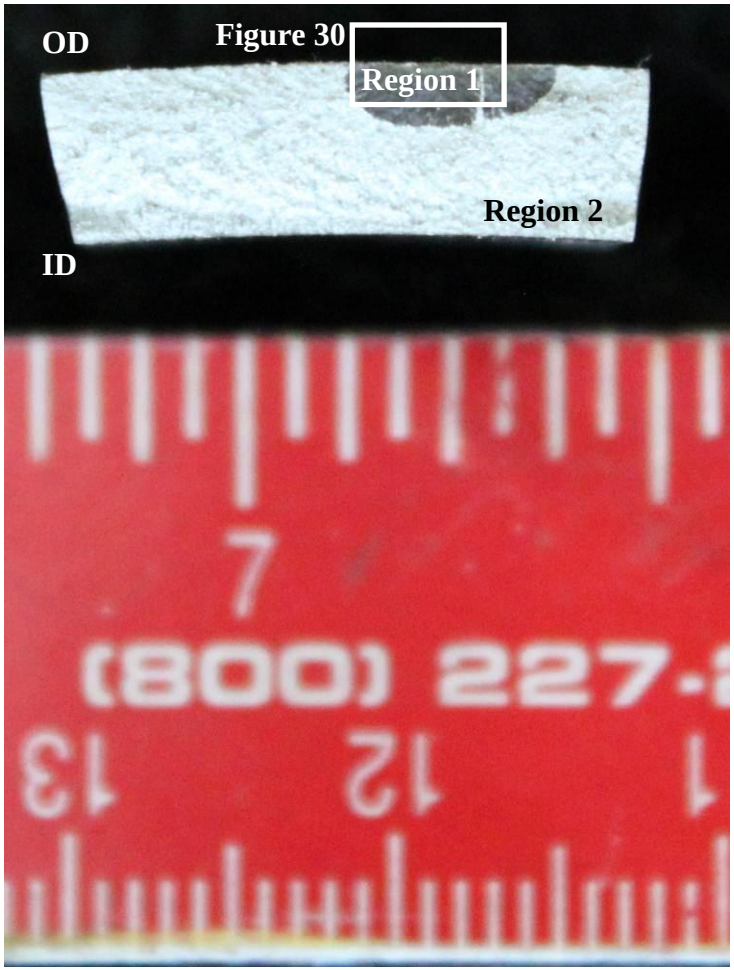

Figure 16. Photograph of the fracture surface from Crack Colony 2.

Figure 17. Photograph of the fracture surface from Crack Colony 3.

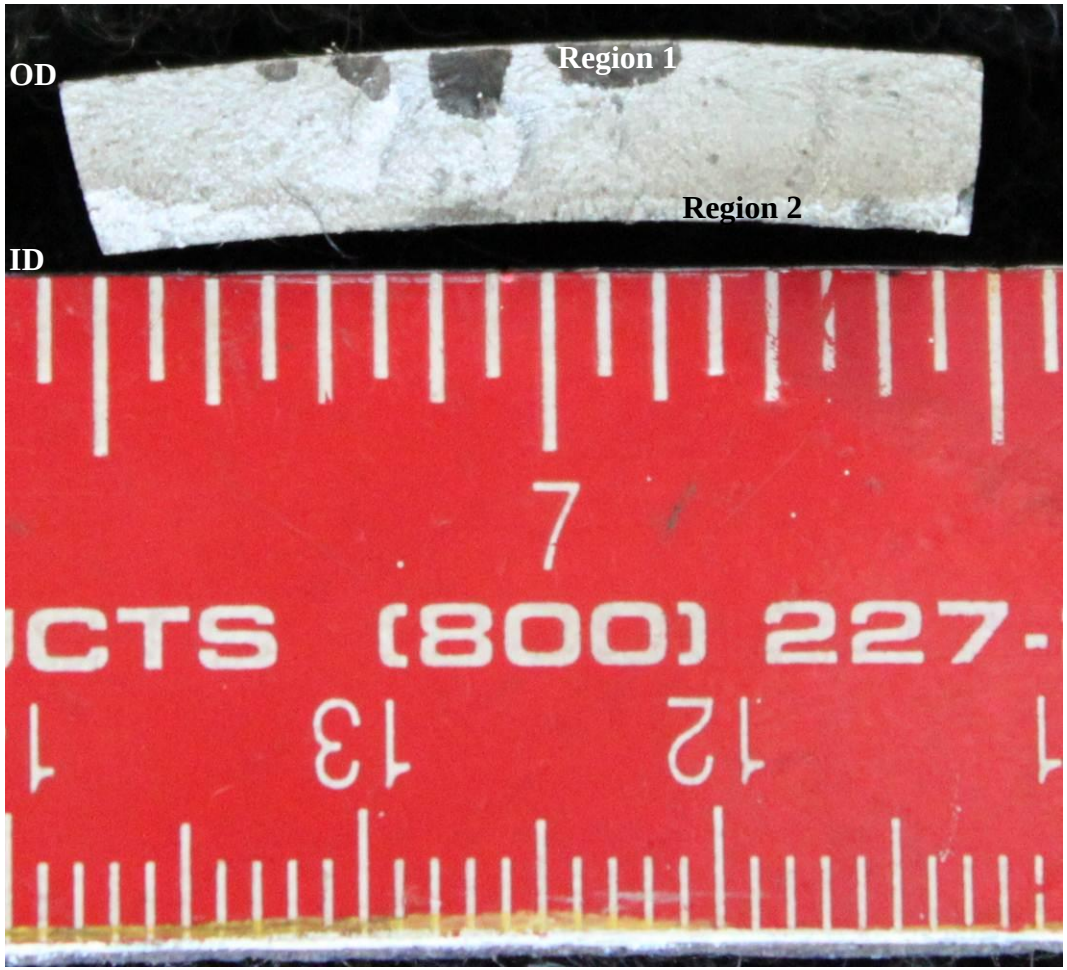

Figure 18. Photograph of the fracture surface from Crack Colony 4.

Figure 19. Photograph of the fracture surface from the feature near Crack Colony 5.

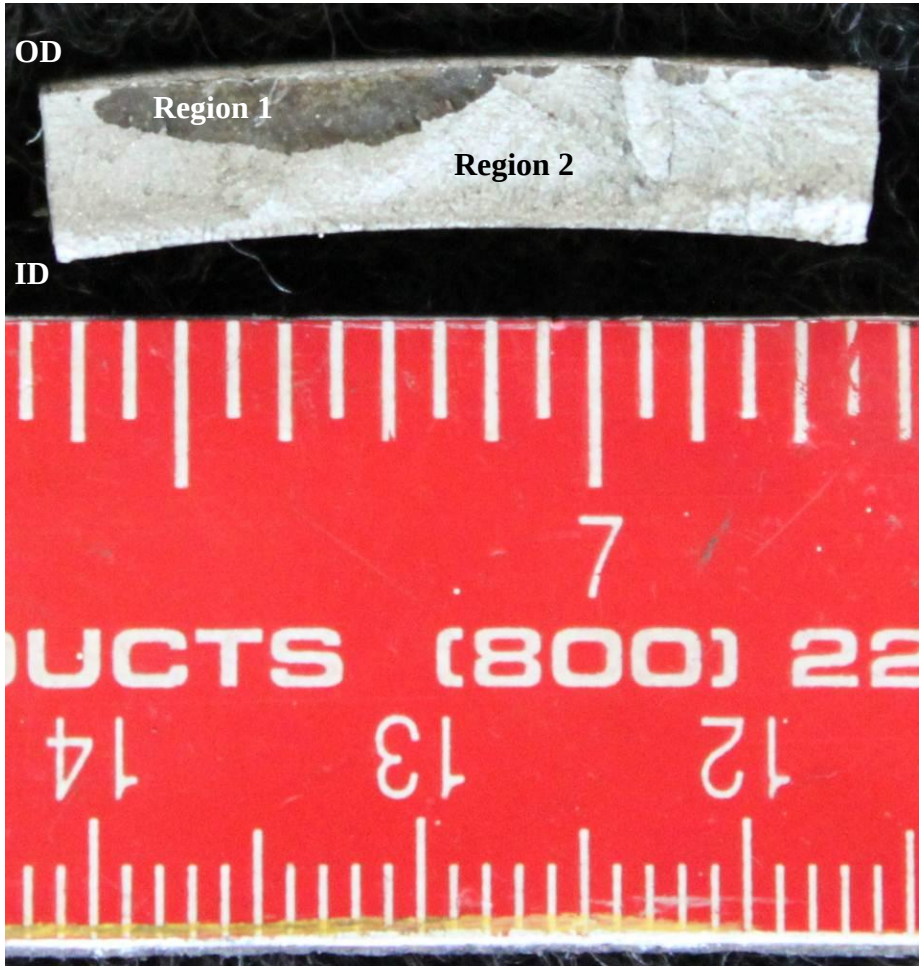

Figure 20. Photograph of the fracture surface from Crack Colony 6.

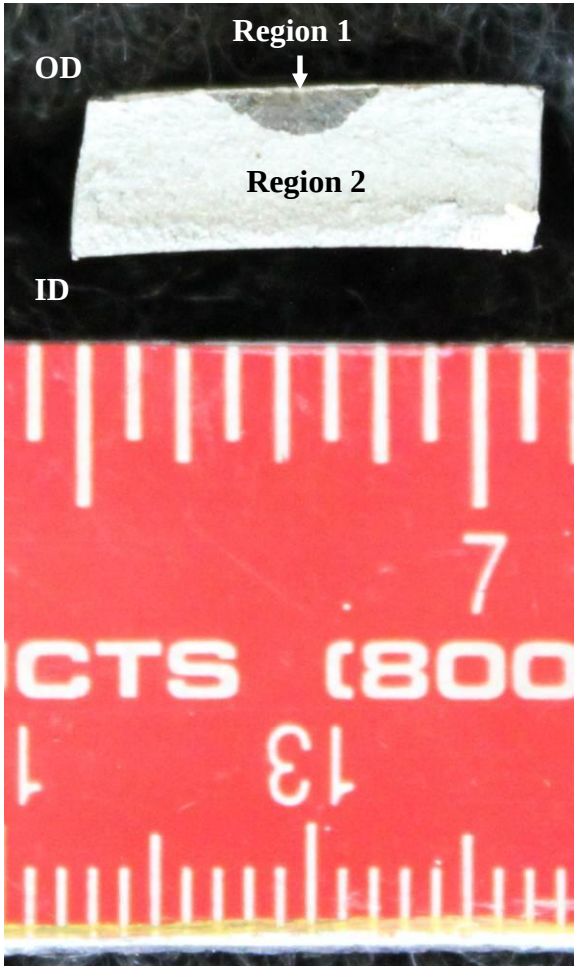

Figure 21. Photograph of the fracture surface from Crack Colony 7.

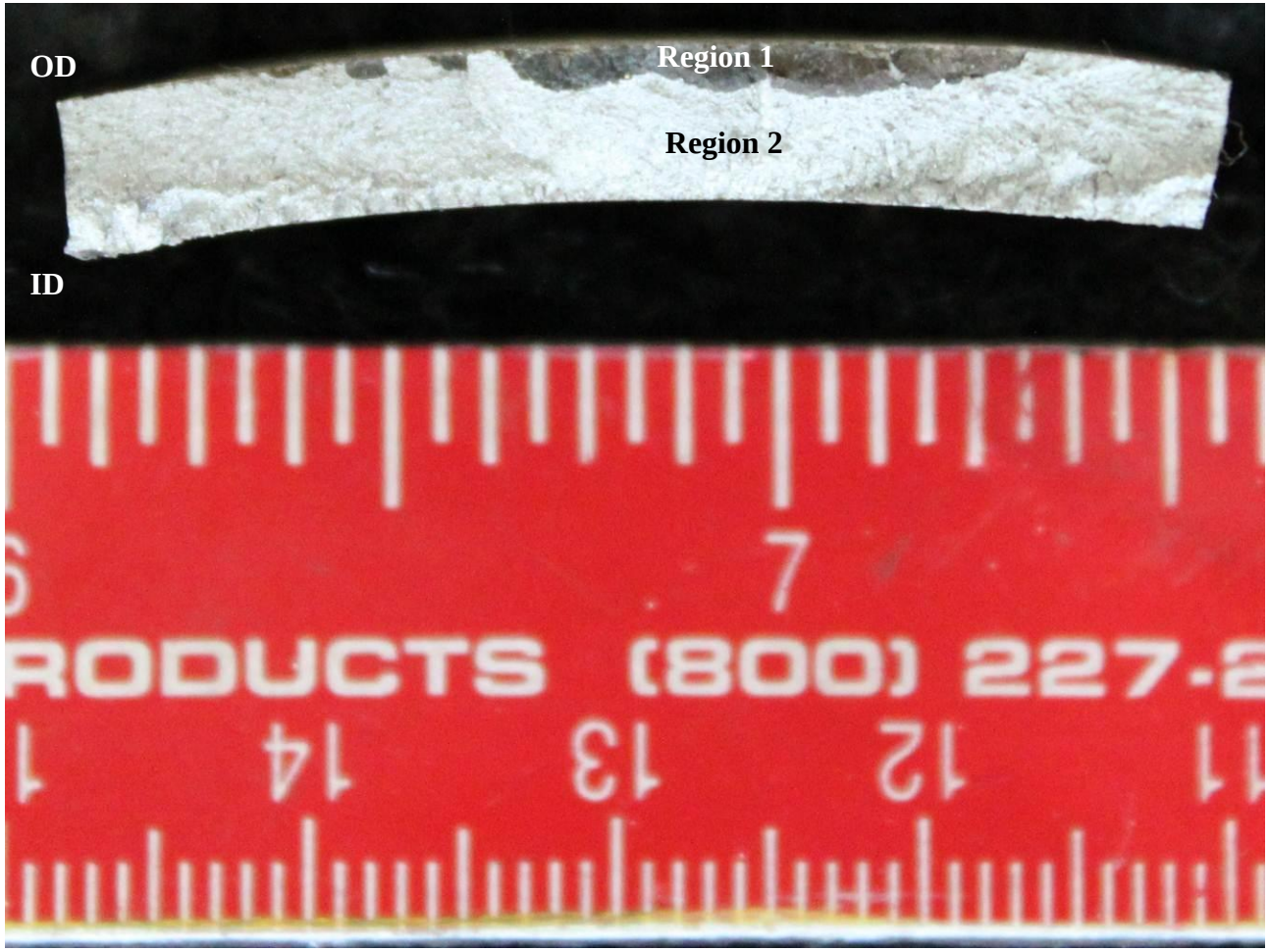

Figure 22. Photograph of the fracture surface from Crack Colony 8A.

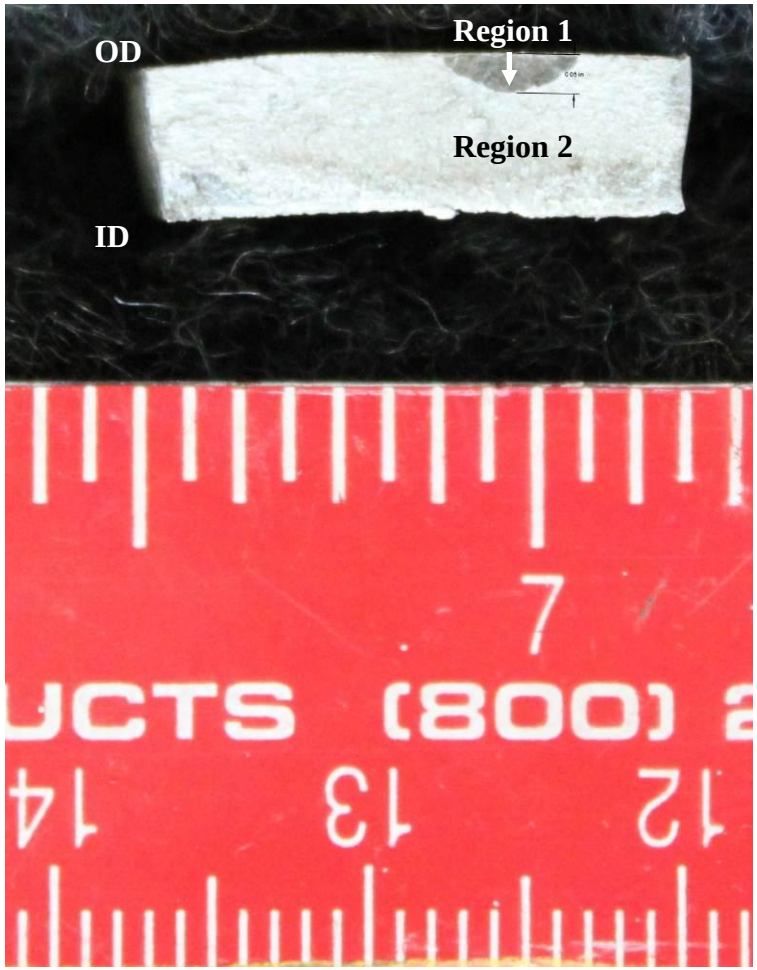

Figure 23. Photograph of the fracture surface from Crack Colony 9B.

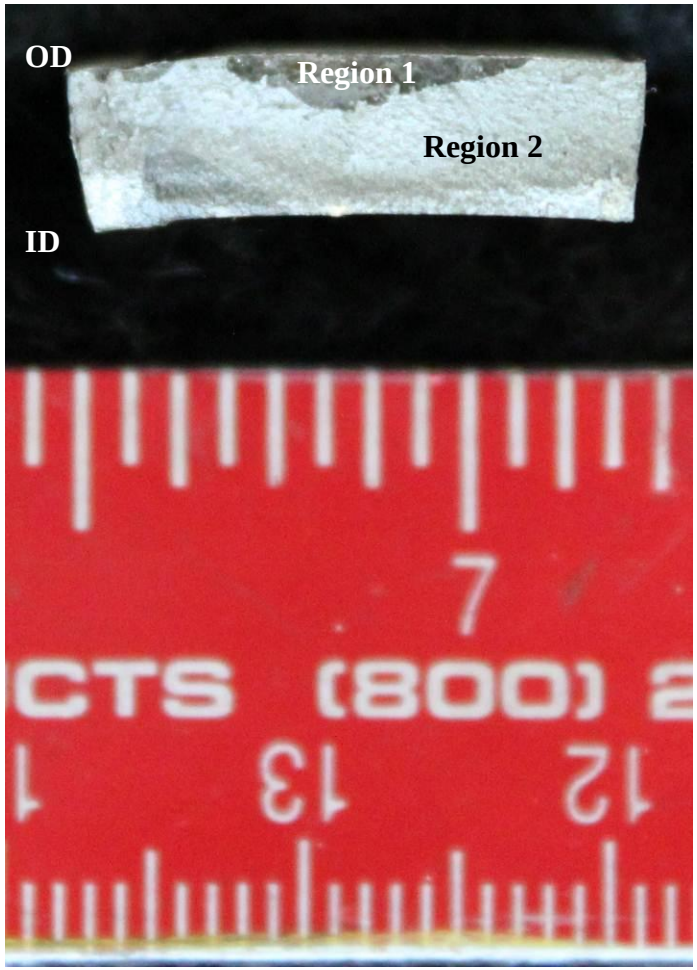

Figure 24. Photograph of the fracture surface from Crack Colony 10.

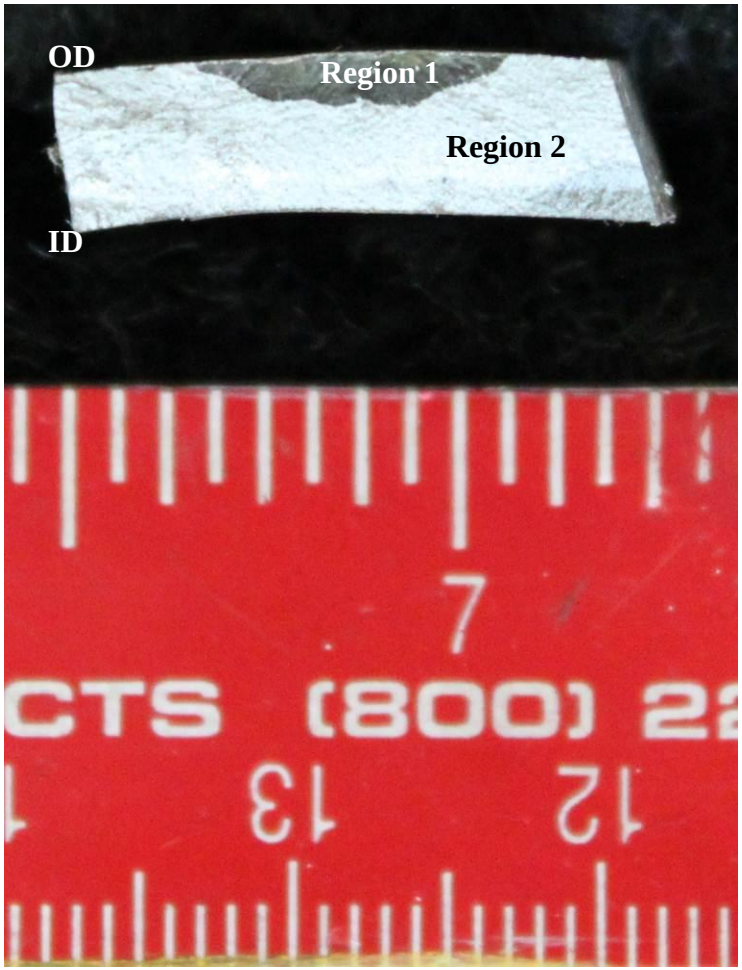

Figure 25. Photograph of the fracture surface from Crack Colony 11.

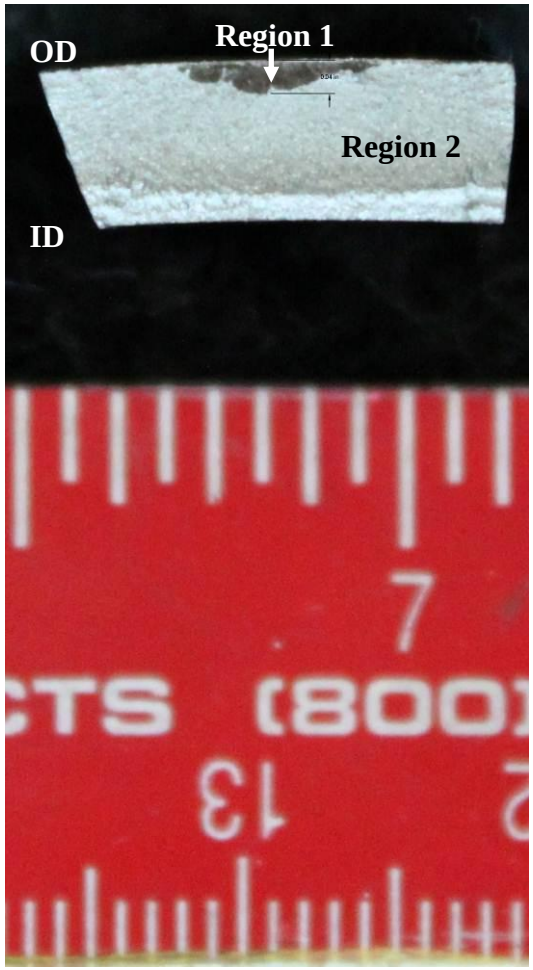

Figure 26. Photograph of the fracture surface from Crack Colony 12.

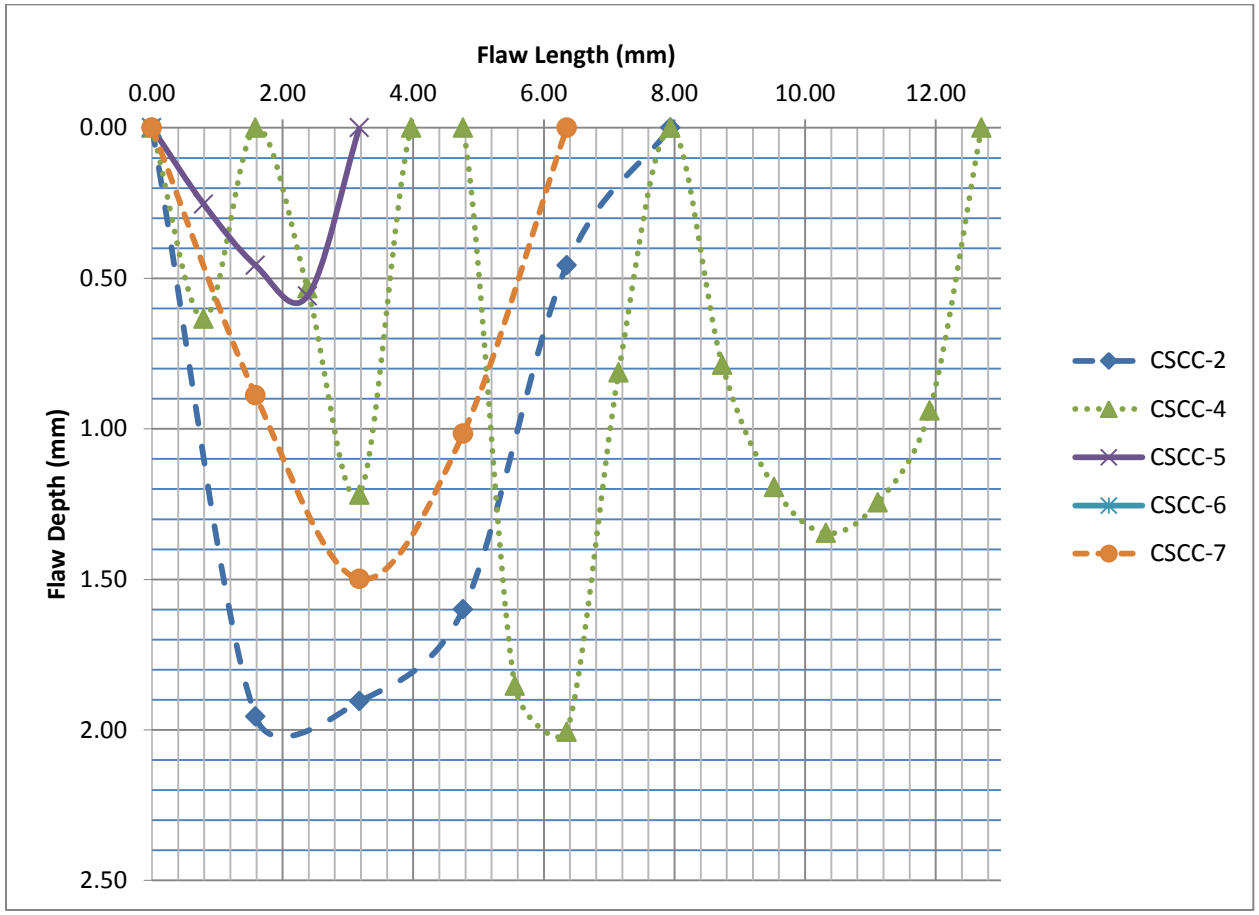

Figure 27. Flaw depth versus flaw length for Crack Colonies 2, 4, 5, 6, and 7.

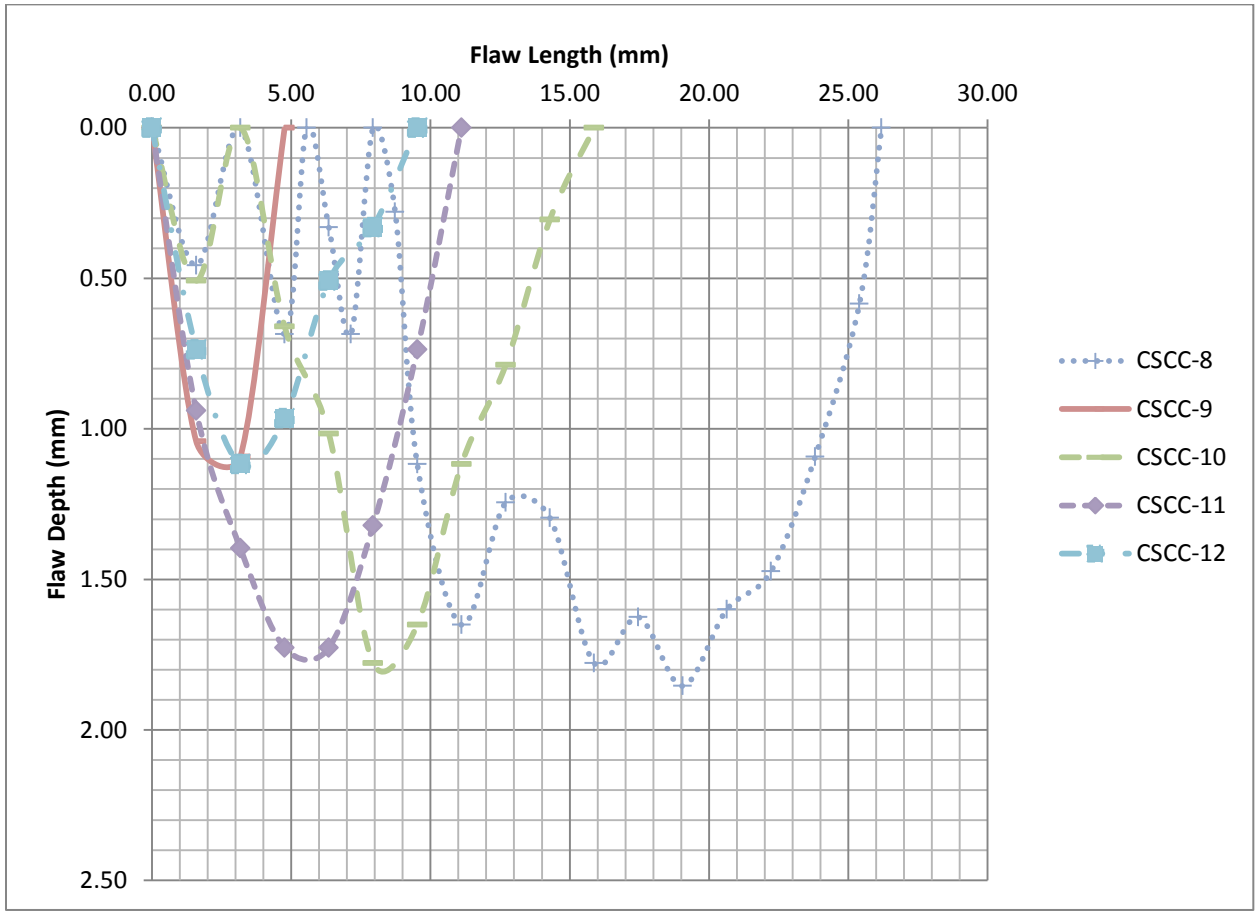

Figure 28. Flaw depth versus flaw length for Crack Colonies 8, 9, 10, 11, and 12.

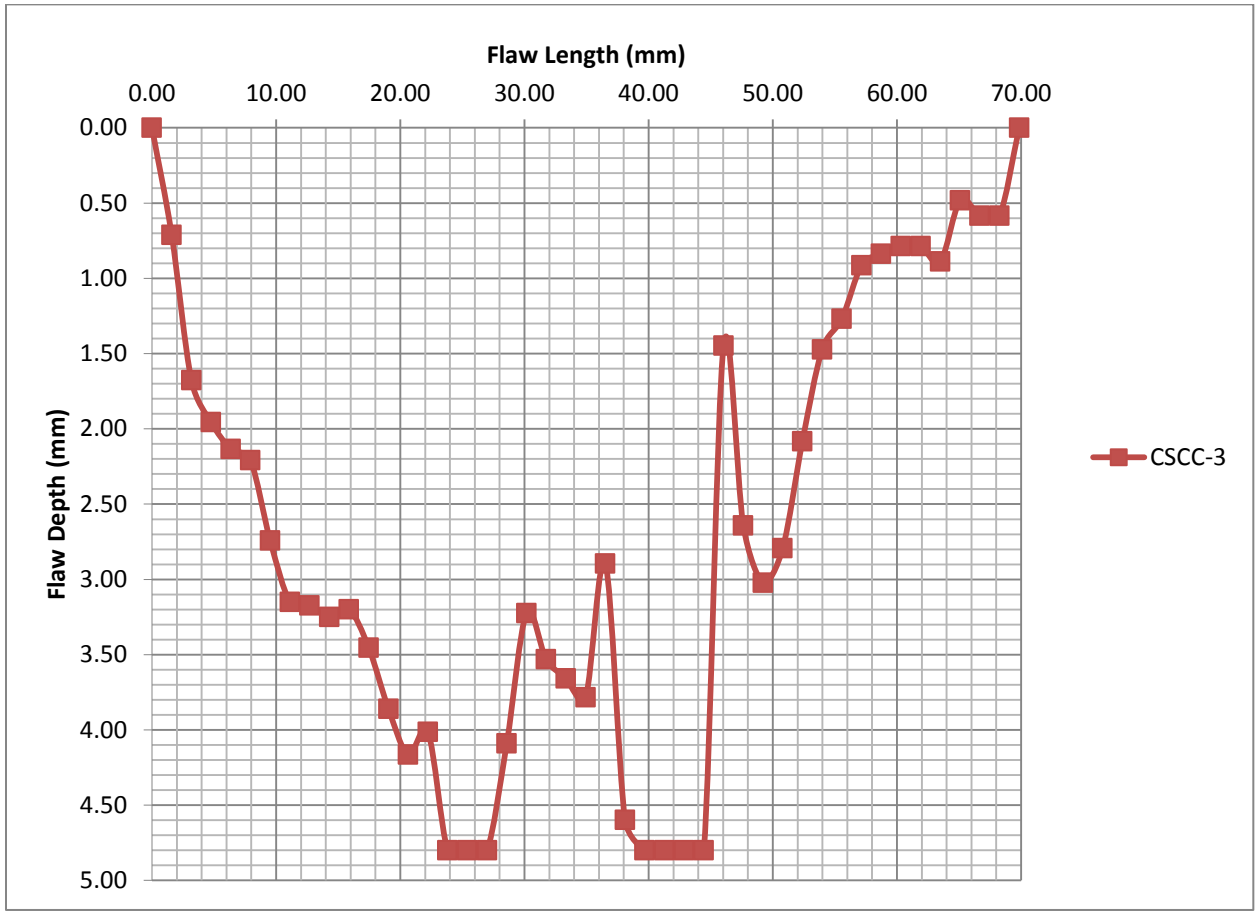

Figure 29. Flaw depth versus flaw length for Crack Colony 3 (at the leak location).

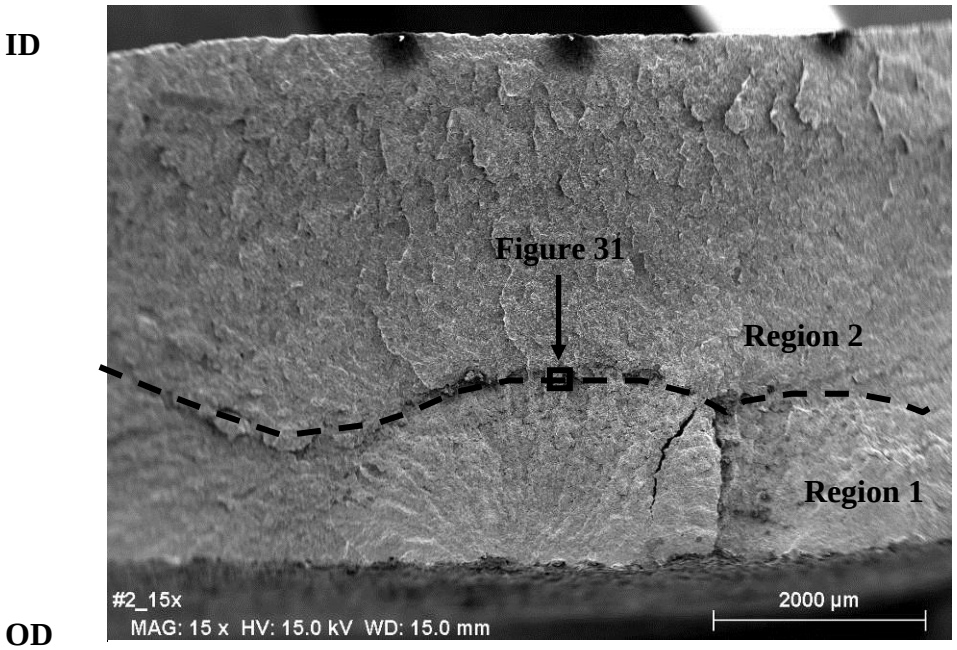

Figure 30. SEM image of fracture surface Sample S1 from Colony 2; mating surface indicated in Figure 16.

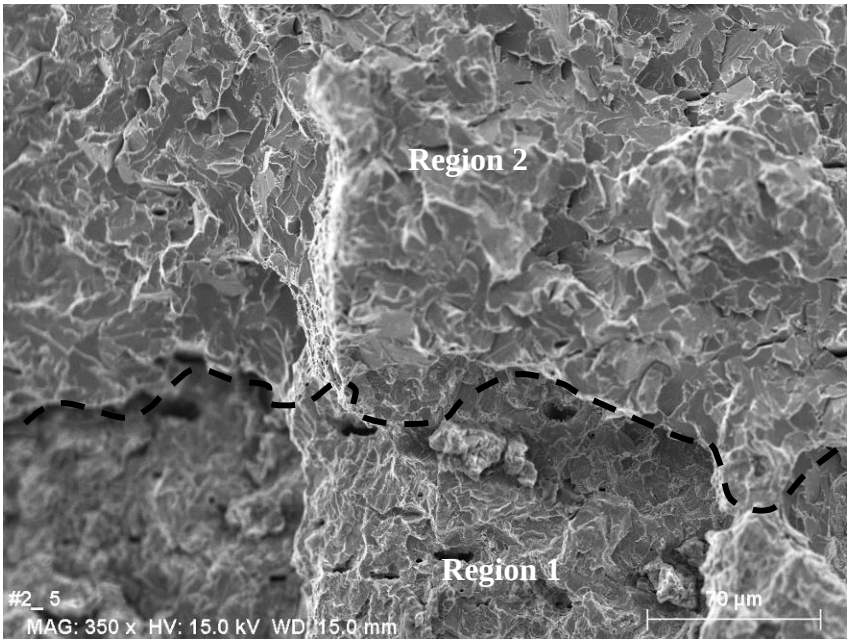

Figure 31. High magnification SEM image of the fracture surface of Sample S1 in the thumbnail crack (Region 1) and brittle overload region (Region 2); area indicated in Figure 30.

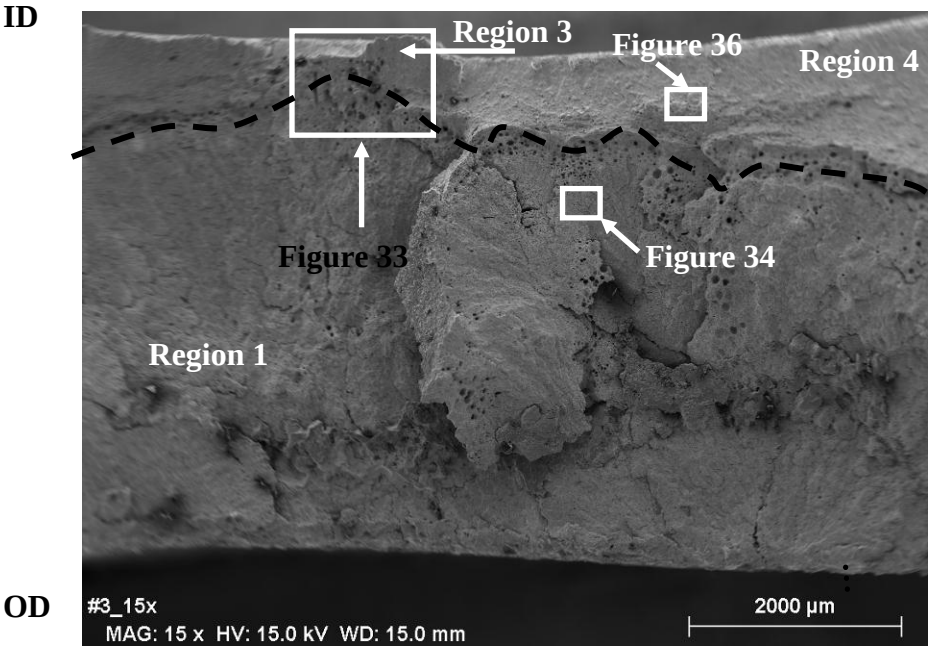

Figure 32. SEM image of fracture surface Sample S2 from Colony 3.

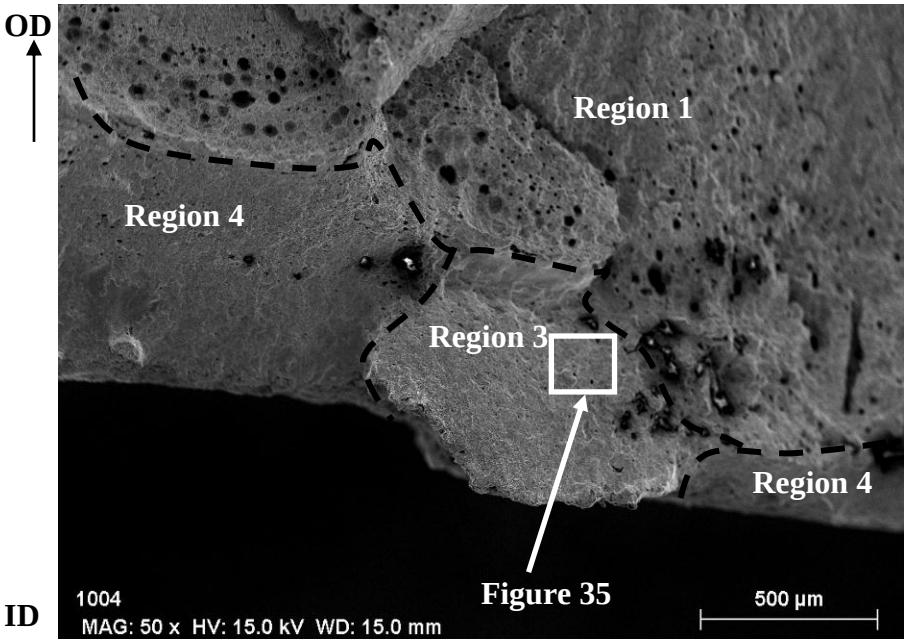

Figure 33. SEM image of the fracture surface of Sample S2 near the ID surface; area indicated in Figure 32.

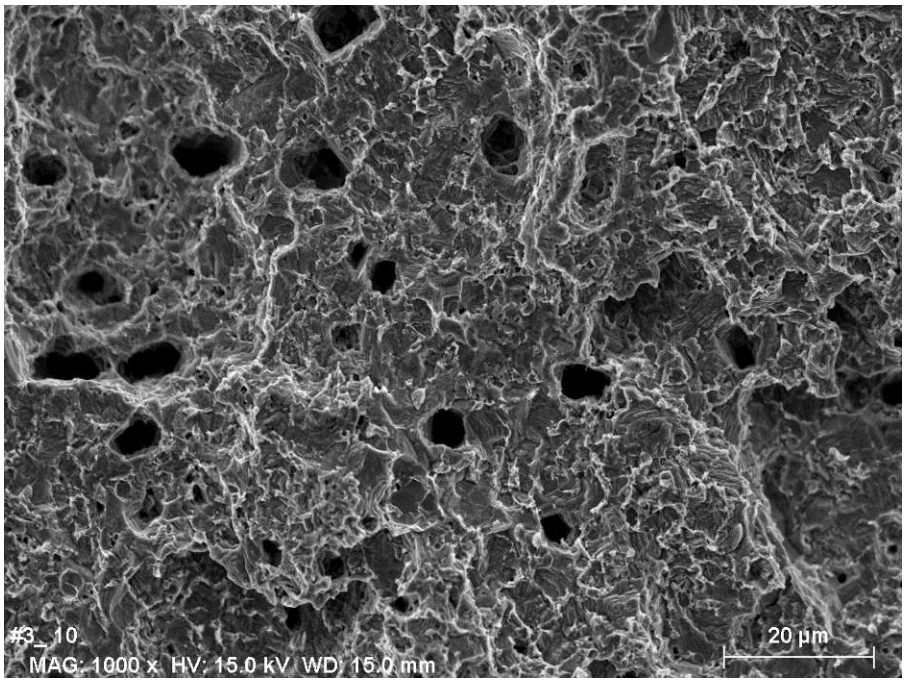

Figure 34. High magnification SEM image of the fracture surface of Sample S2 in the thumbnail crack region (Region 1); area indicated in Figure 32.

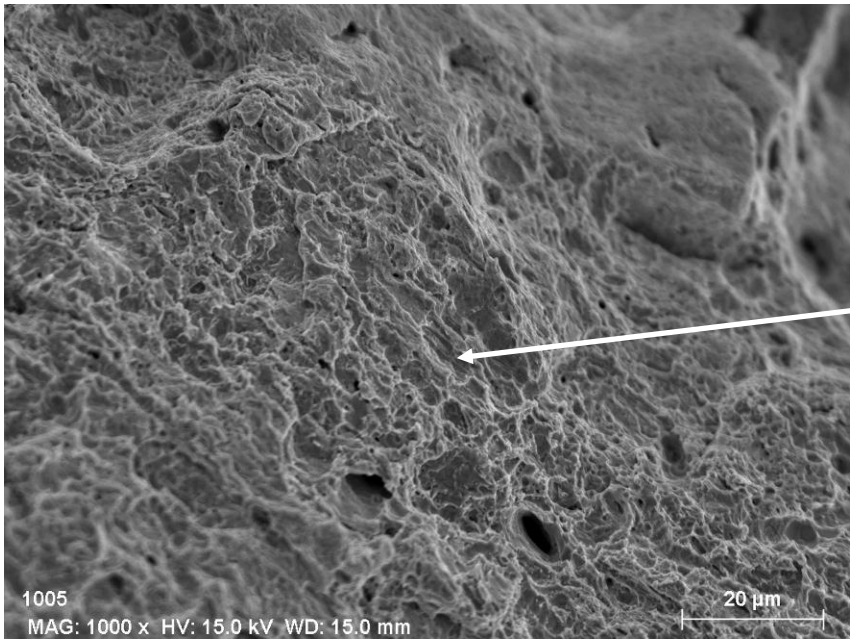

Figure 35. High magnification SEM image of the fracture surface of Sample S2 near the ID surface; area indicated in Figure 33.

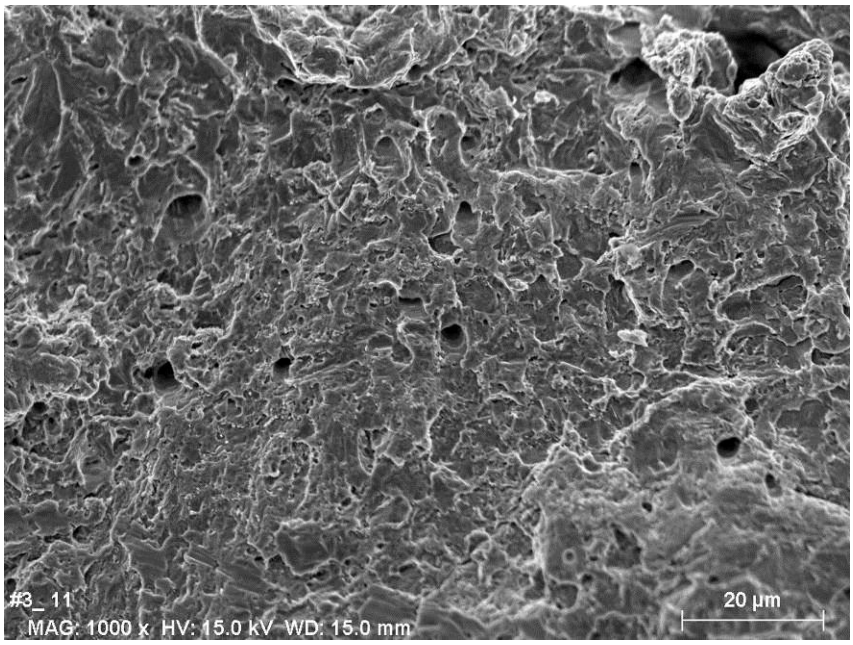

Figure 36. High magnification SEM image of the fracture surface of Sample S2 outside of the thumbnail crack region (Region 4); area indicated in Figure 33.

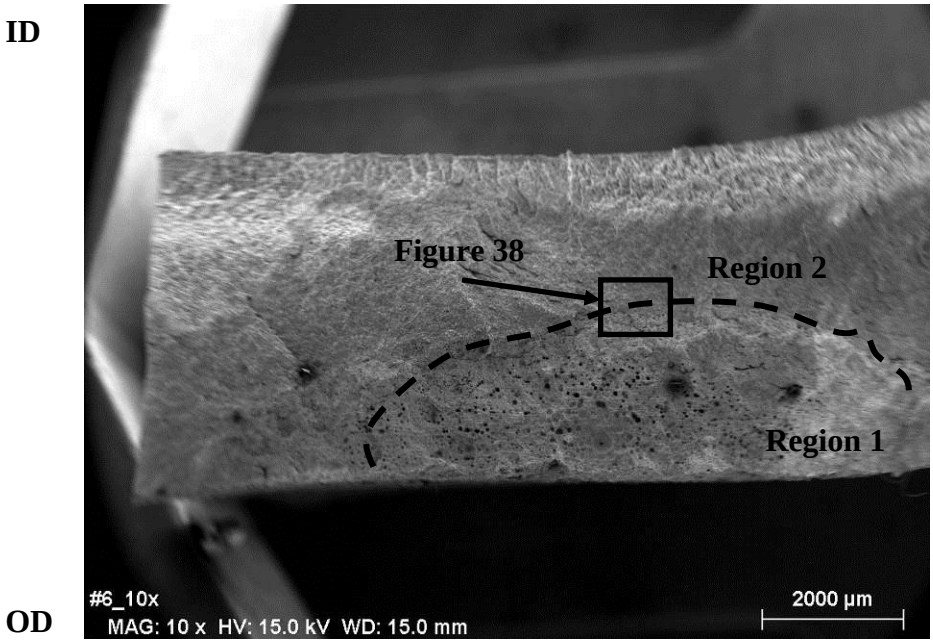

Figure 37. SEM image of fracture surface Sample S3 from Colony 6; area indicated in Figure 20.

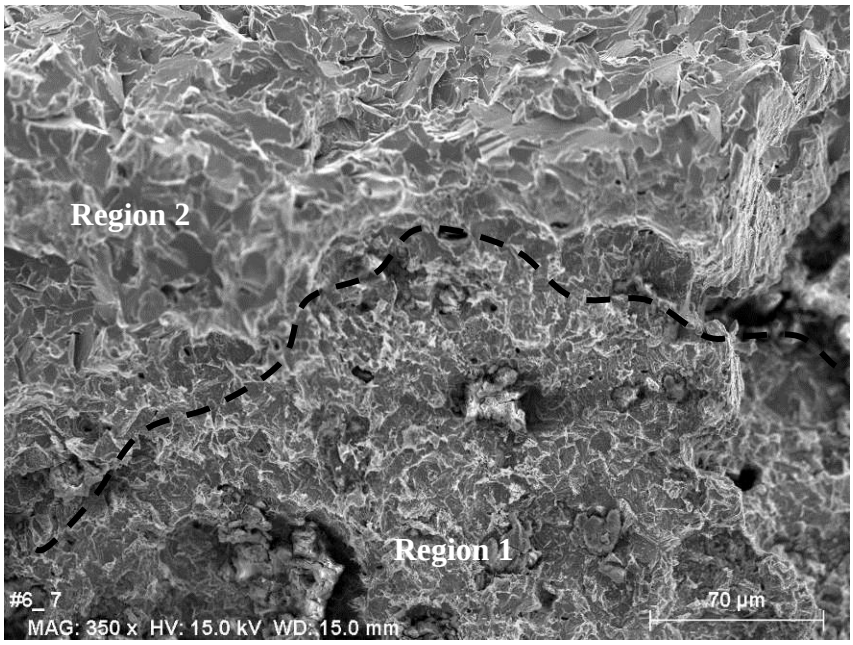

Figure 38. SEM image of the fracture surface of Sample S4 at the thumbnail crack region (Region 1) and laboratory fracture region (Region 2); area indicated in Figure 37.

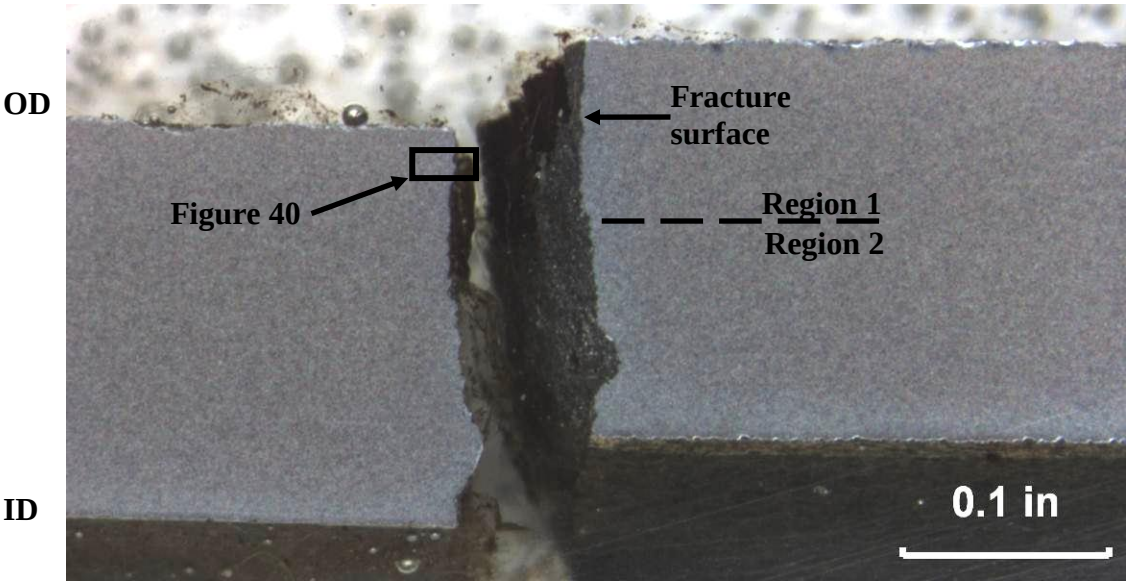

Figure 39. Stereo light photomicrograph of Mount M1 (4% Nital Etchant). Mount was removed from Crack Colony 2.

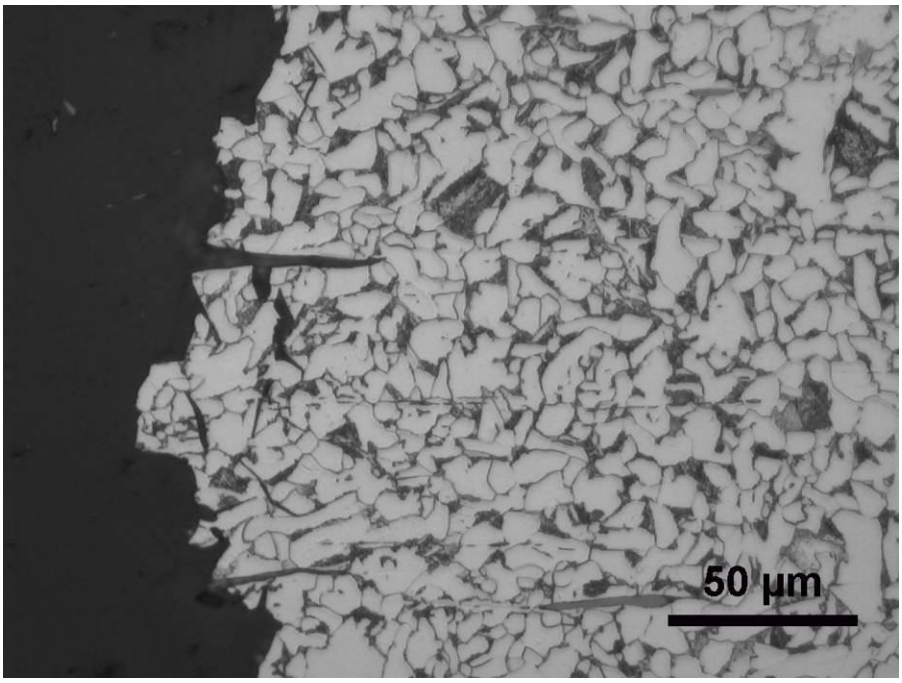

Figure 40. Close-up photomicrograph of Mount M1 (4% Nital Etchant); mirror image of area indicated in Figure 39.

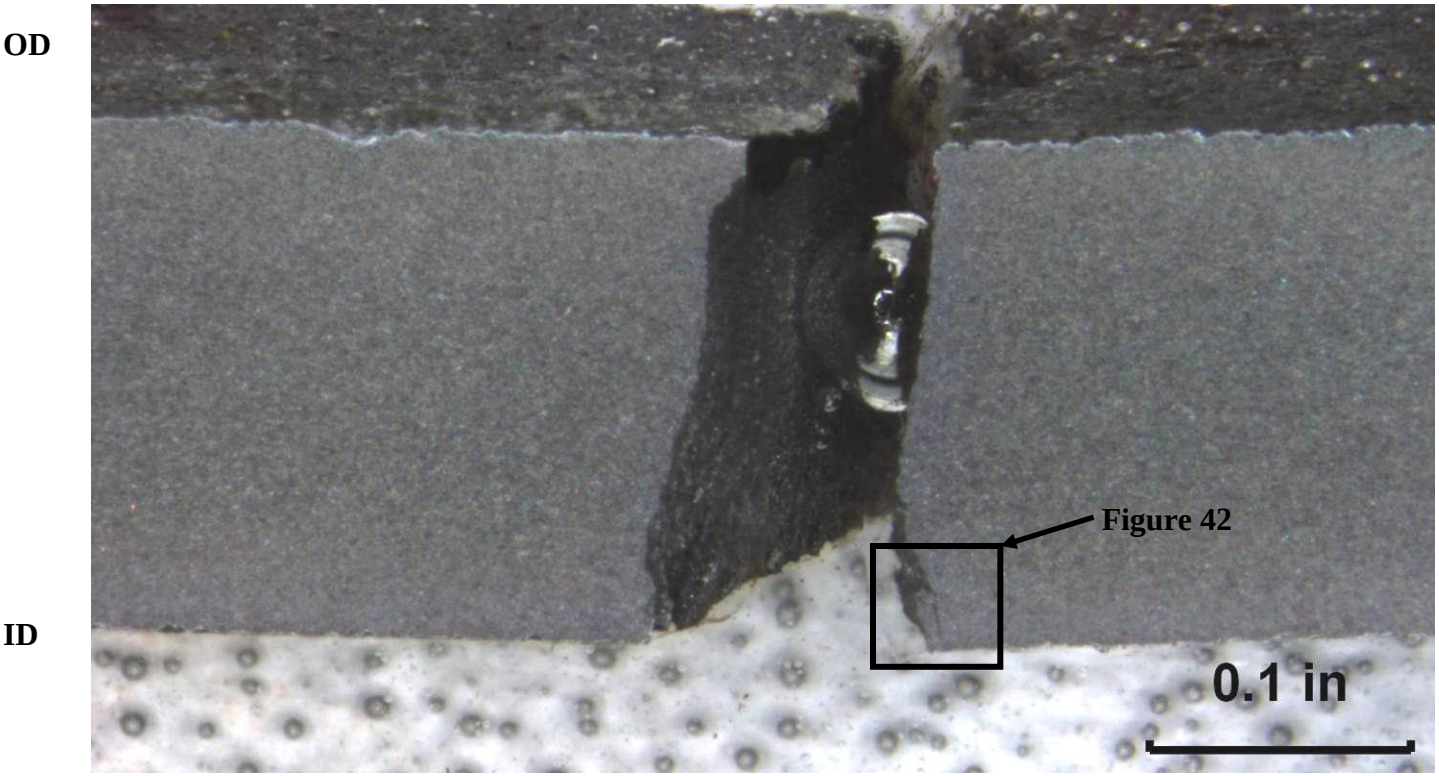

Figure 41. Stereo light photomicrograph of Mount M2 (4% Nital Etchant). Mount was removed from Crack Colony 3 (leak location).

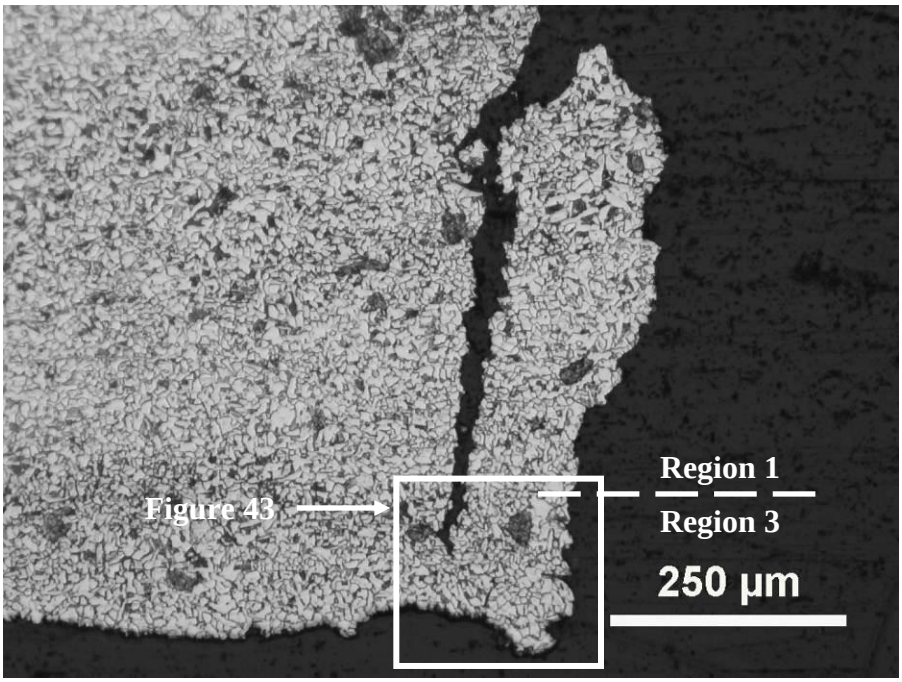

Figure 42. Stereo light photomicrograph of Mount M2 near the ID surface (4% Nital Etchant); mirror image of area indicated in Figure 41.

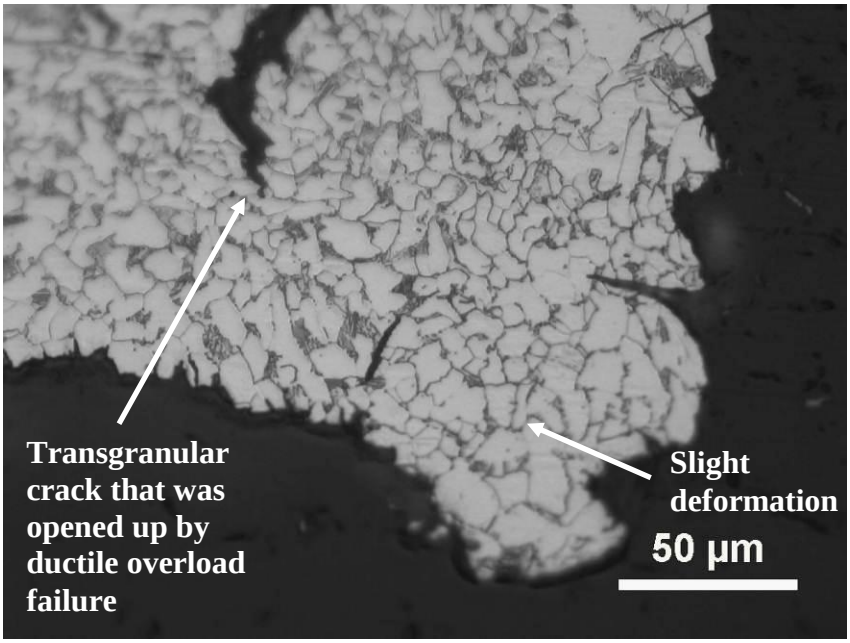

Figure 43. Close-up photomicrograph of Mount M2 near the ID surface (4% Nital Etchant); area indicated in Figure 42.

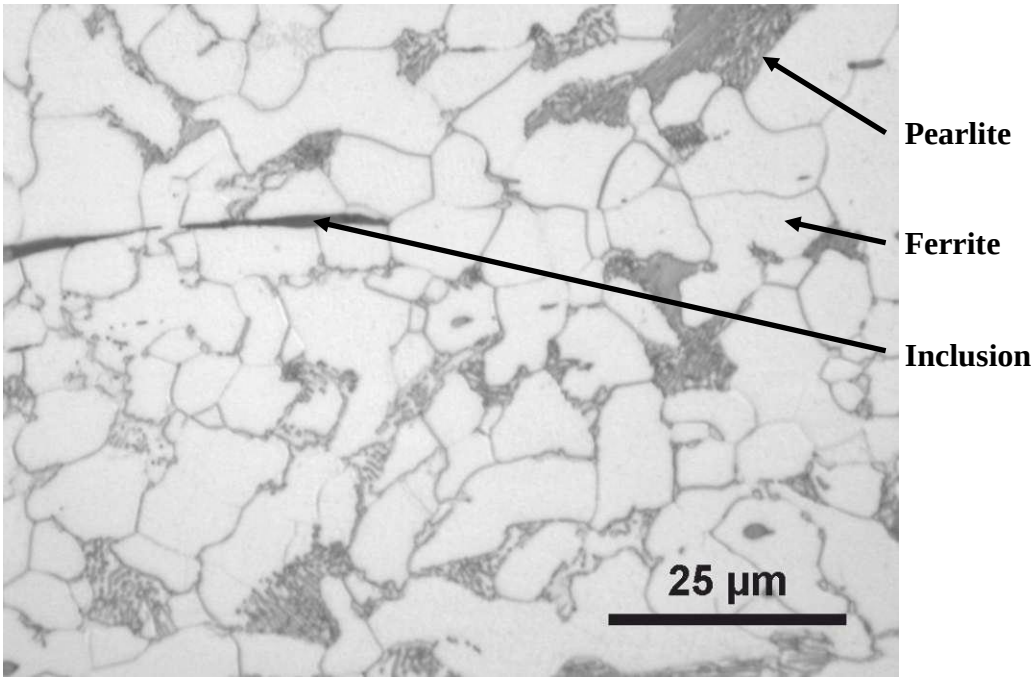

Figure 44. Light photomicrograph of the typical base metal microstructure (Mount M2, 4% Nital Etchant).

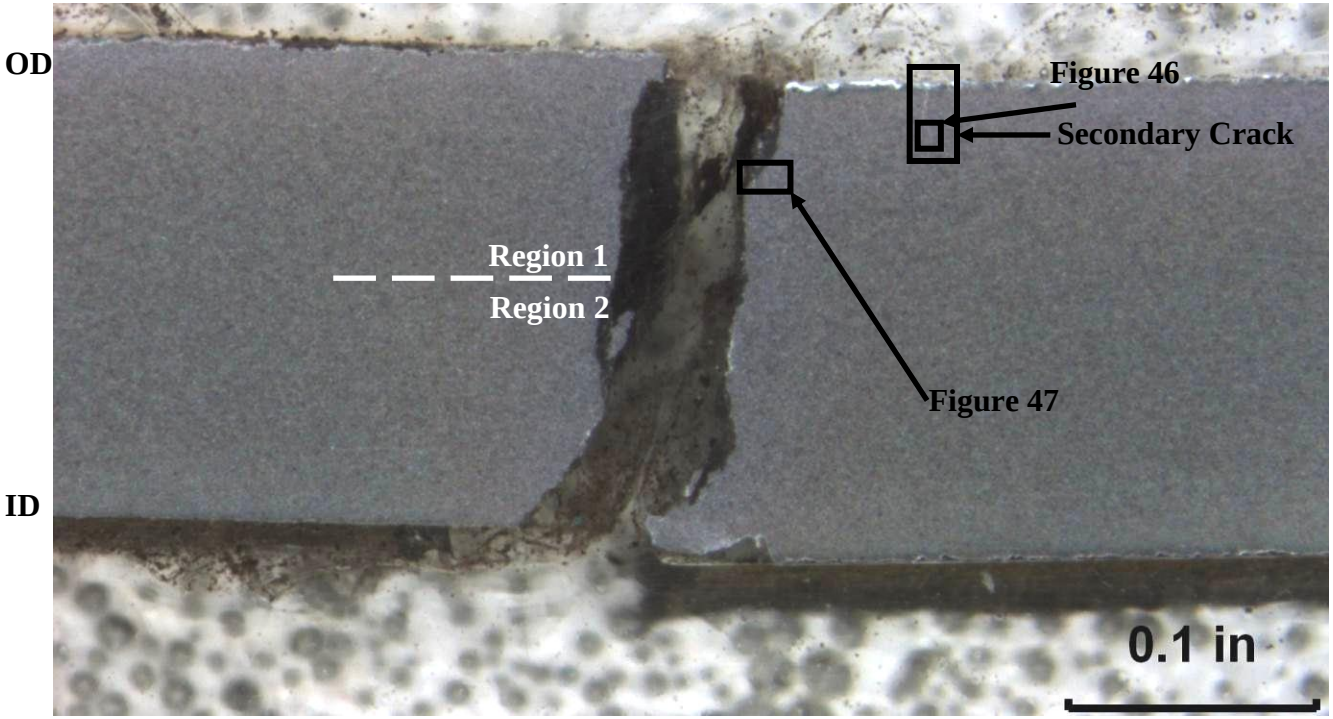

Figure 45. Stereo light photomicrograph of Mount M3 (4% Nital Etchant). Mount was removed from Crack Colony 6.

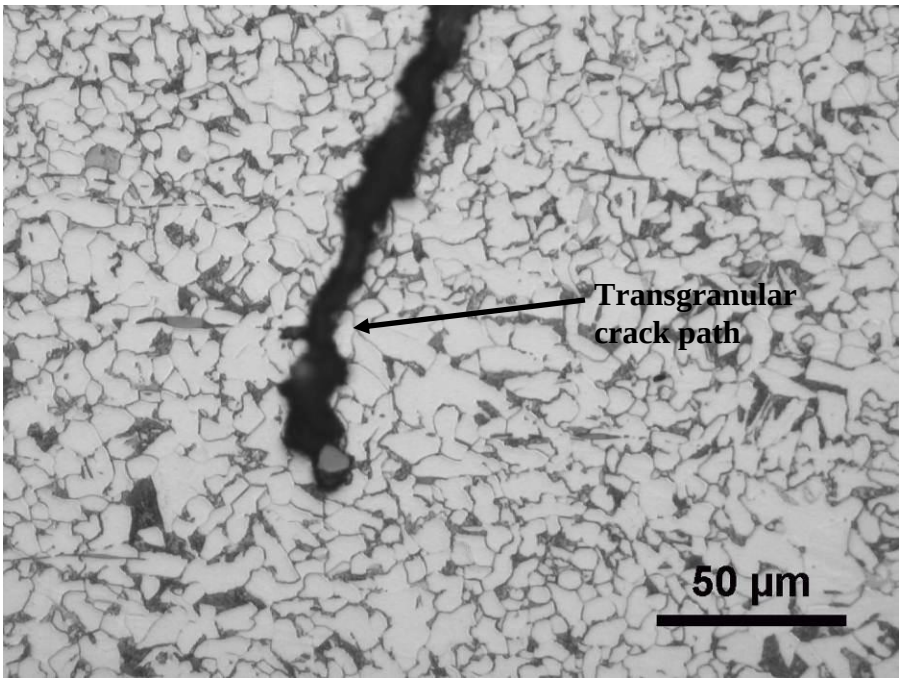

Figure 46. Close-up photomicrograph of Mount M3 showing a crack tip (4% Nital Etchant); area indicated in Figure 45.

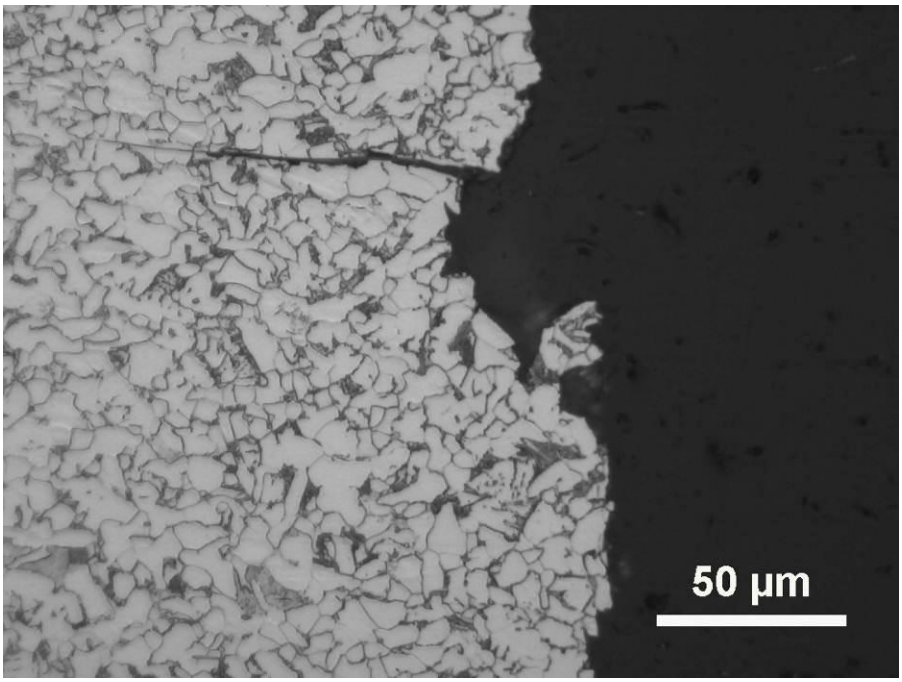

Figure 47. Light photomicrograph of Mount M3 (4% Nital Etchant); mirror image of area indicated in Figure 45.

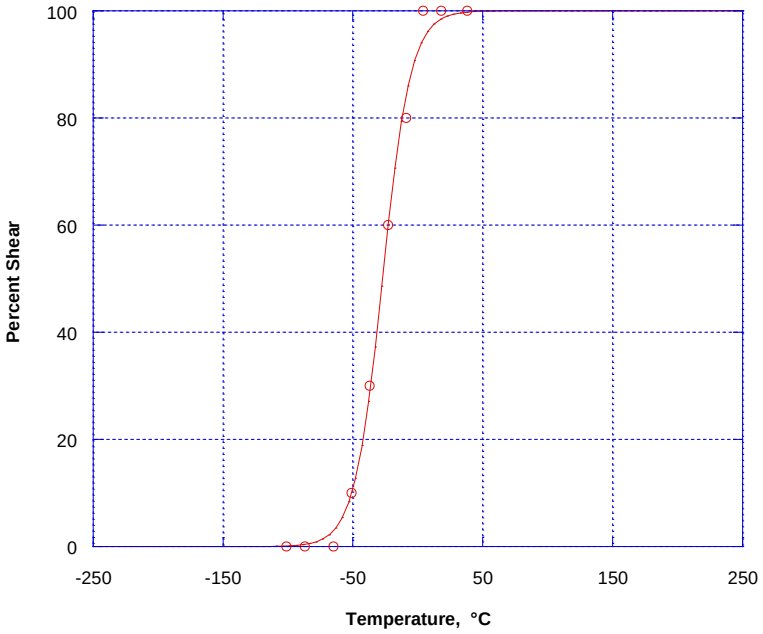

Figure 48. Percent shear from Charpy V-notch tests as a function of temperature for axial base metal samples removed from the pipe section.

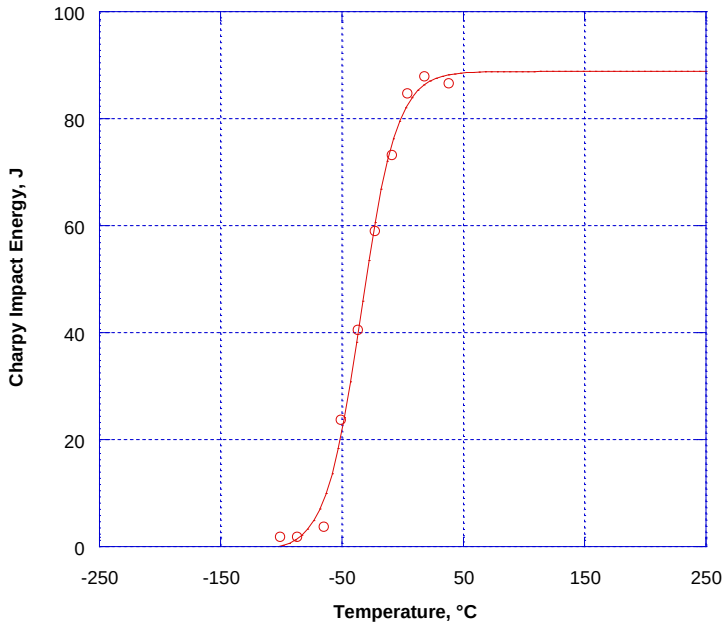

Figure 49. Charpy V-notch impact energy as a function of temperature for axial base metal samples removed from the pipe section.

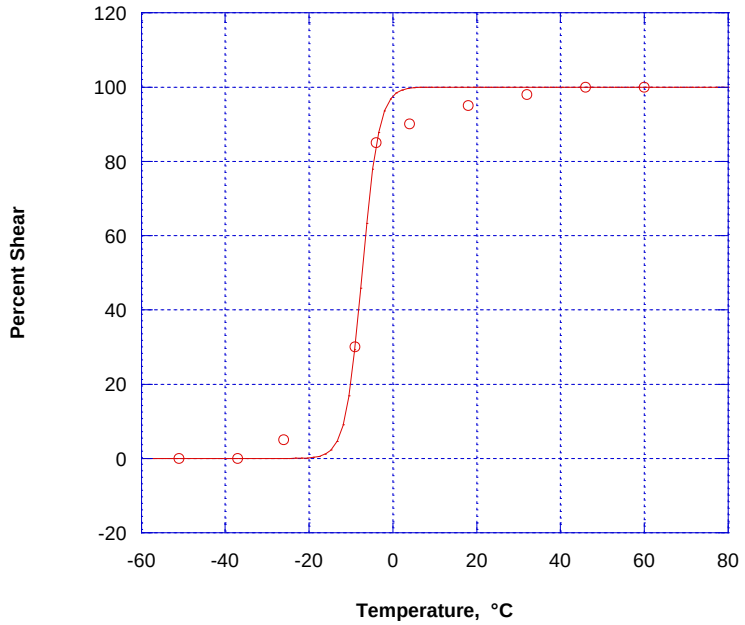

Figure 50. Percent shear from Charpy V-notch tests as a function of temperature for transverse base metal samples removed from the pipe section.

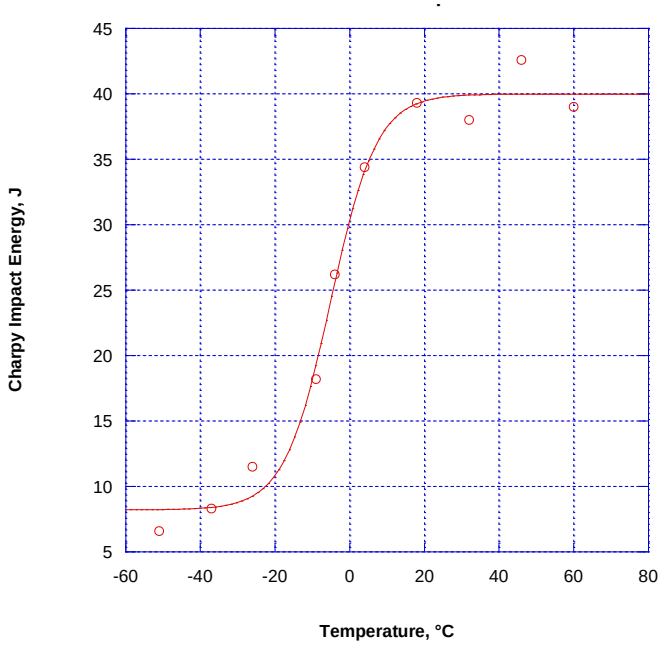

Figure 51. Charpy V-notch impact energy as a function of temperature for transverse base metal samples removed from the pipe section.

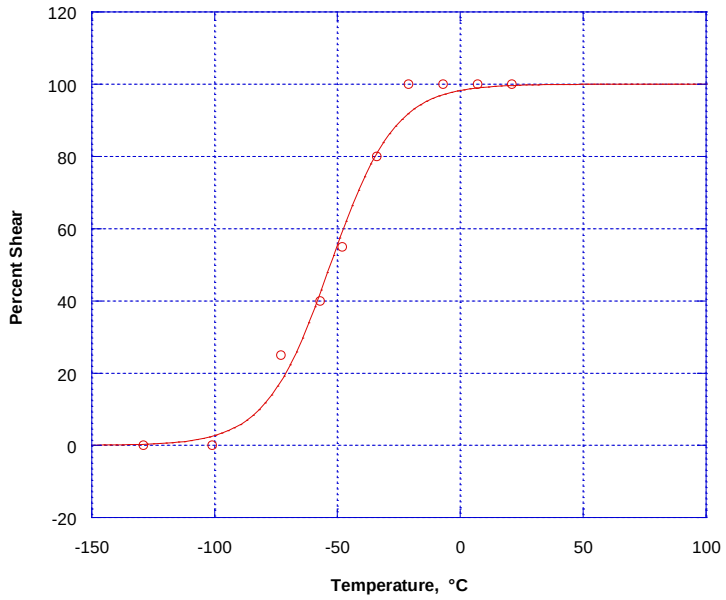

Figure 52. Percent shear from Charpy V-notch tests as a function of temperature for axial seam weld samples removed from the pipe section.

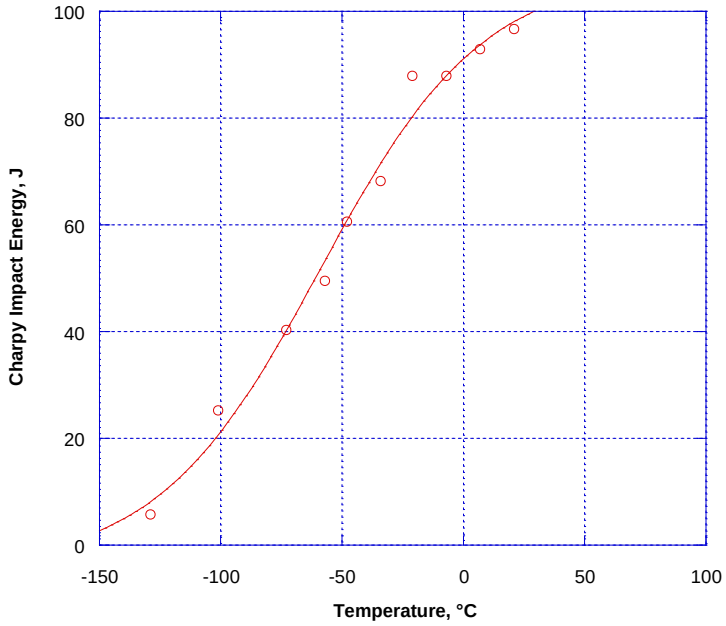

Figure 53. Charpy V-notch impact energy as a function of temperature for axial seam weld samples removed from the pipe section.

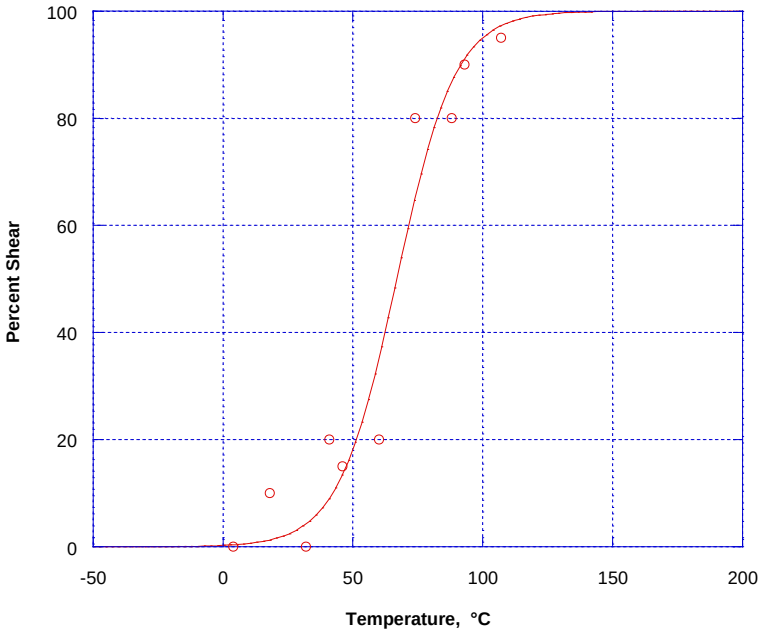

Figure 54. Percent shear from Charpy V-notch tests as a function of temperature for transverse seam weld samples removed from the pipe section.

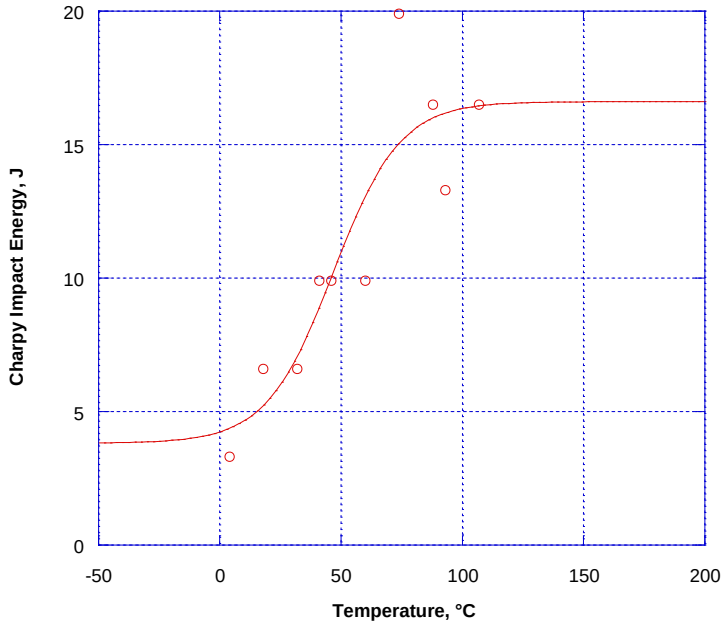

Figure 55. Charpy V-notch impact energy as a function of temperature for transverse seam weld samples removed from the pipe section.

Det Norske Veritas

Det Norske Veritas (DNV) is a leading, independent provider of services for managing risk with a global presence and a network of 300 offices in 100 different countries. DNV's objective is to safeguard life, property and the environment.

DNV assists its customers in managing risk by providing three categories of service: classification, certification, and consultancy. Since establishment as an independent foundation in 1864, DNV has become an internationally recognized provider of technical and managerial consultancy services and one of the world's leading classification societies. This means continuously developing new approaches to health, safety, quality, and environmental management, so businesses can run smoothly in a world full of surprises.

Global Impact for a Safe and Sustainable Future

Learn more on www.dnv.com